IL-33 promotes the egress of group 2 innate lymphoid cells from the bone marrow

Matthew T. Stier,[1] Jian Zhang,[2] Kasia Goleniewska,[2] Jacqueline Y. Cephus,[2] Mark Rusznak,[2] Lan Wu,[1] Luc Van Kaer,[1] Baohua Zhou,[3] Dawn C. Newcomb,[1,2] and R. Stokes Peebles Jr.[1,2]

[1]Department of Pathology, Microbiology, and Immunology and [2]Division of Allergy, Pulmonary and Critical Care Medicine, Department of Medicine, Vanderbilt University Medical Center, Nashville, TN
[3]Wells Center for Pediatric Research, Department of Pediatrics, Indiana University School of Medicine, Indianapolis, IN

Group 2 innate lymphoid cells (ILC2s) are effector cells within the mucosa and key participants in type 2 immune responses in the context of allergic inflammation and infection. ILC2s develop in the bone marrow from common lymphoid progenitor cells, but little is known about how ILC2s egress from the bone marrow for hematogenous trafficking. In this study, we identified a critical role for IL-33, a hallmark peripheral ILC2-activating cytokine, in promoting the egress of ILC2 lineage cells from the bone marrow. Mice lacking IL-33 signaling had normal development of ILC2s but retained significantly more ILC2 progenitors in the bone marrow via augmented expression of CXCR4. Intravenous injection of IL-33 or pulmonary fungal allergen challenge mobilized ILC2 progenitors to exit the bone marrow. Finally, IL-33 enhanced ILC2 trafficking to the lungs in a parabiosis mouse model of tissue disruption and repopulation. Collectively, these data demonstrate that IL-33 plays a critical role in promoting ILC2 egress from the bone marrow.

INTRODUCTION

Innate lymphoid cells (ILCs) are mucosal effector cells that are derived from common lymphoid progenitors (CLPs). They are embedded at environmental interfaces, where they can respond rapidly and directly in an antigen-independent manner to a wide array of insults. Subsets of ILCs—groups 1, 2, and 3—mirror the adaptive $CD4^+$ T helper lymphocyte lineages Th1, Th2, and Th17, respectively, in regard to their transcriptional governance and cytokine production (Klose and Artis, 2016; background on ILC reviewed in Morita et al., 2016). Group 2 ILCs (ILC2s) require GATA3 (Hoyler et al., 2012; Mjösberg et al., 2012) and produce abundant quantities of IL-5, IL-13, and/or IL-9 and, under certain circumstances, IL-4, similar to $CD4^+$ Th2 cells (Moro et al., 2010; Neill et al., 2010; Price et al., 2010; Wilhelm et al., 2011; Doherty et al., 2013). Known activators of ILC2s include IL-33, IL-25, thymic stromal lymphopoietin (TSLP), TNF family member TL1A, and lipid mediators such as prostaglandin D_2 and leukotriene D_4 (Moro et al., 2010; Neill et al., 2010; Halim et al., 2012; Doherty et al., 2013; Xue et al., 2014; Yu et al., 2014). ILC2s have been implicated directly in the pathogenesis of inflammatory diseases in animal models or humans including asthma (Bartemes et al., 2012, 2014; Halim et al., 2012; Christianson et al., 2015), atopic dermatitis (Kim et al., 2013; Salimi et al., 2013), chronic rhinosinusitis (Mjösberg et al., 2011; Shaw et al., 2013), viral infection (Chang et al., 2011; Jackson et al., 2014), and helminth infection (Moro et al., 2010; Neill et al., 2010; Price et al., 2010). Additionally, ILC2s regulate tissue homeostasis, including epithelial repair (Monticelli et al., 2011, 2015) and healthy adipose tissue maintenance (Molofsky et al., 2013; Brestoff et al., 2015; Lee et al., 2015).

Our understanding of ILC2 egress from developmental sites such as the bone marrow and subsequent trafficking to tissues is highly limited. The establishment of ILC2 niches in the periphery occurs in the perinatal period. For instance, seeding of the lungs occurs within the first 2 wk of life in an IL-33–dependent manner (de Kleer et al., 2016; Saluzzo et al., 2017; Steer et al., 2017). After colonization, maintenance of ILC2 populations in mucosal tissues is thought to occur by multiple mechanisms. Intrinsically, ILC2s are long lived in the tissue (Nussbaum et al., 2013). Under steady-state conditions, data suggest that ILC2s are replenished from ILC2 or ILC2 lineage progenitor cells that are in situ within these peripheral tissues (Gasteiger et al., 2015; O'Sullivan et al., 2016). However, in the context of protracted type 2 inflammation such as *Nippostrongylus brasiliensis* infection, ILC2s are in part reseeded hematogenously, likely from sources such as the bone marrow (Gasteiger et al., 2015). Moreover, myeloablation and reconstitution with donor bone marrow leads to a significant accumulation of donor ILC2s in classically ILC2-rich sites, including the colon and skin in humans (Vély et al., 2016). Collectively, these data implicate both peripheral and central mechanisms in the maintenance of ILC2 frequencies in peripheral tissues, particularly in the context of initial tissue seeding and disrupted tissue homeostasis.

Correspondence to R. Stokes Peebles Jr.: stokes.peebles@vanderbilt.edu

The Rockefeller University Press
J. Exp. Med. 2018 Vol. 215 No. 1 263–281
https://doi.org/10.1084/jem.20170449

Development of ILC2s in the bone marrow has been the subject of intense interest. Thematically, our understanding of ILC2 development has focused largely on critical transcriptional regulators such as Bcl11b and ETS1 (Walker et al., 2015;Yu et al., 2015; Zook et al., 2016; and reviewed in Zook and Kee, 2016). However, the role of extracellular signals in ILC2 development remains more poorly defined. Mice deficient in the *Il7r* or *Il2r* have markedly reduced numbers of ILC2s, suggesting a critical role for these cytokines in ILC2 development and/or homeostasis (Moro et al., 2010; Wong et al., 2012). An in vitro system for the differentiation of CLPs to ILC2s requires IL-7, Notch ligand, and IL-33 (Wong et al., 2012; Xu et al., 2015). IL-33 is a hallmark activator of ILC2s in peripheral tissues, and the most mature ILC2 lineage cell in the bone marrow, referred to as the ILC2 progenitor (ILC2P), expresses the IL-33 receptor ST2 (Hoyler et al., 2012; Spooner et al., 2013). However, a role for IL-33 in ILC2 lineage development or trafficking in vivo remains unknown.

We sought to understand the role of IL-33, a quintessential peripheral activator of ILC2s, in bone marrow ILC2 lineage development and trafficking. *Il33*$^{-/-}$ and *St2*$^{-/-}$ mice had significantly increased numbers of ILC2Ps in the bone marrow and reduced numbers of ILC2s in peripheral tissues compared with WT mice. Lack of IL-33 signaling precipitated critical changes in the chemokine receptor profile of ILC2Ps. Notably, ILC2Ps in *St2*$^{-/-}$ mice expressed higher levels of CXCR4, which stimulated the retention of ILC2Ps in the bone marrow. Finally, sublethal radiation exposure in parabiotic mice established a key role for IL-33–responsive hematogenous trafficking of ILC2s in the setting of disrupted tissue homeostasis. Collectively, these data implicate IL-33 as a key driver of bone marrow ILC2 lineage cell egress.

RESULTS

Deficiency in IL-33 signaling promotes the accumulation of ILC2Ps in the bone marrow

IL-33 signaling via its receptor ST2 is a central pathway for the activation of ILC2 effector functions in peripheral tissues. Moreover, IL-33 has been used in vitro to stimulate the differentiation of ILC2s from CLPs (Wong et al., 2012; Xu et al., 2015). We hypothesized that IL-33 promotes the development of ILC2s in vivo. Accordingly, we assayed for the number of ILC2Ps in the bone marrow of naive BALB/c WT, *Il33*$^{-/-}$, and *St2*$^{-/-}$ mice. ILC2Ps and peripheral ILC2s were defined as viable cells that were CD45^{+} Lin^{-} IL-25R^{+} CD25^{+} CD127^{+} (Fig. 1 A). WT, *Il33*$^{-/-}$, and *St2*$^{-/-}$ mice had similar numbers of total cells in the bone marrow (Fig. 1 B), but unexpectedly, we identified a significant increase in the frequency and total number of ILC2Ps in *Il33*$^{-/-}$ and *St2*$^{-/-}$ mice compared with WT mice (Fig. 1, A, C, and D). A similar increase in the total number of bone marrow ILC2Ps was observed in *Il33*$^{-/-}$ mice on a C57BL/6 background, indicating that this phenotype was independent of host genetic background (Fig. 1 E). We next characterized the number of ILC2s in peripheral tissues. We focused on ILC2-rich tissues, specifically the lungs, skin, and mesenteric lymph nodes (mLNs). In contrast to our result in the bone marrow, we found a significant decrease in the frequency and total number of ILC2s in the lungs and skin of *Il33*$^{-/-}$ and *St2*$^{-/-}$ mice compared with WT mice, and a significant decrease in the frequency and total number of ILC2s in the mLNs of *St2*$^{-/-}$ mice compared with WT mice (Fig. 2). This phenotype of accumulation in the bone marrow in *Il33*$^{-/-}$ and *St2*$^{-/-}$ mice was unique to ILC2s among major ST2-expressing cell types, as eosinophil, basophil, and mast cell lineages did not exhibit increased frequency in the bone marrow of *St2*$^{-/-}$ mice (Fig. S1 A). Fewer eosinophils were recovered from the lungs and skin of *St2*$^{-/-}$ mice, likely secondary to the reduction of ILC2s in these tissues (Fig. S1, B and C; Nussbaum et al., 2013). These data suggested that IL-33 might affect ILC2P egress from the bone marrow.

In addition to IL-33, TSLP is a potent activator of ILC2s. However, these two cytokines act via distinct cellular pathways. IL-33 binds to ST2 to induce MyD88 activation and NF-κB translocation to the nucleus, whereas TSLP binds to a heterodimer of the TSLPR and IL-7Rα and activates STAT5 (reviewed in Bartemes and Kita, 2012). We assessed whether the effects on ILC2P/ILC2 frequency were unique to IL-33 signaling or were part of a broader network of ILC2-activating cytokines that functioned redundantly. We measured the number of ILC2Ps in the bone marrow and ILC2s in the lungs of WT and *Tslpr*$^{-/-}$ mice. In contrast to mice lacking IL-33 signaling, the loss of TSLPR signaling reduced the frequency and total number of ILC2Ps in the bone marrow (Fig. S2, A–D) and ILC2s in the lungs (Fig. S2, E–H) compared with WT mice. These data indicate that IL-33 acts distinctly from other ILC2-activating cytokines in regulating bone marrow ILC2P frequency and that TSLP may instead play an important role in ILC2 development.

IL-33 deficiency does not appreciably alter the hallmark functional capacities of ILC2Ps

We considered whether the increase in ILC2P frequency might be a compensatory effect for reduced proliferative potential or cytokine-producing capacity of ILC2Ps in *Il33*$^{-/-}$ and *St2*$^{-/-}$ mice. ILC2Ps from the bone marrow of WT and *Il33*$^{-/-}$ mice were enriched by magnetic selection for lineage negative cells, purified by FACS, and cultured with IL-2 alone or IL-2 plus IL-33. ILC2Ps from *Il33*$^{-/-}$ mice have developed in the absence of IL-33 but have an intact *St2* gene locus and are poised to respond to IL-33. Thus, we were able to consider the developmental role of IL-33 on the proliferative capacity and cytokine expression of ILC2Ps.

Before culture, we stained ILC2Ps with CellTrace Violet to measure proliferation. After 5 d of in vitro culture, we harvested ILC2Ps for flow cytometric analysis of CellTrace Violet dye dilution (Fig. 3 A). For both WT and *Il33*$^{-/-}$ ILC2Ps, IL-2 alone did not induce proliferation. IL-2 and IL-33 in combination induced robust proliferation as measured by serial dye dilution in both WT and *Il33*$^{-/-}$ ILC2Ps. Importantly,

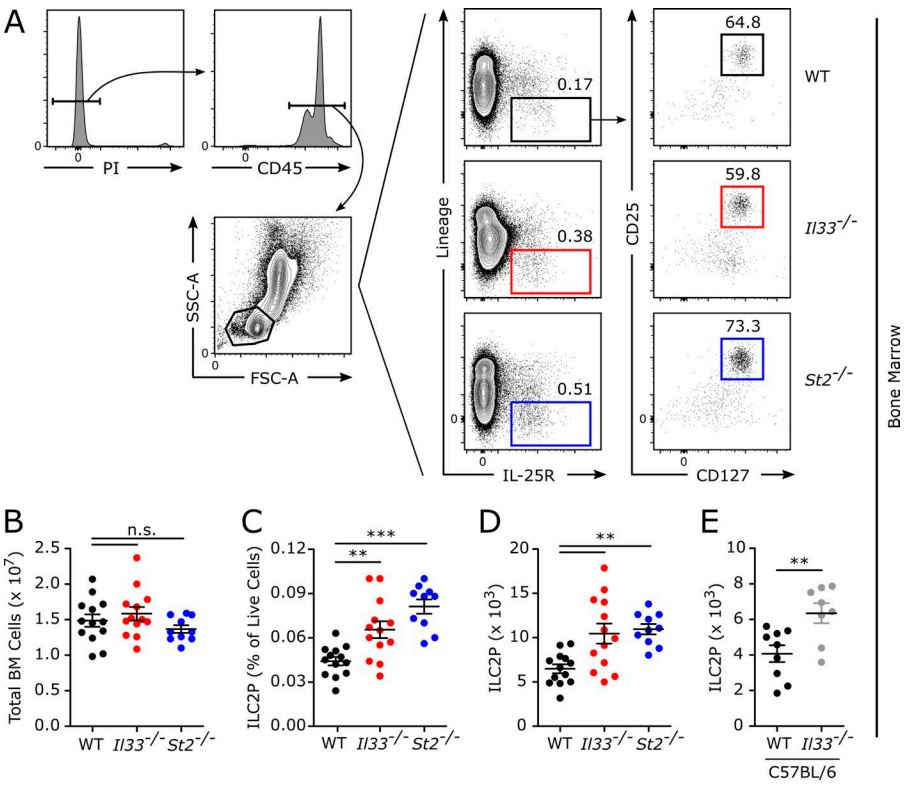

Figure 1. **Deficiency in IL-33 signaling leads to an accumulation of ILC2Ps in the bone marrow.** Adult naive WT BALB/c, *Il33*$^{-/-}$, and *St2*$^{-/-}$ mice were killed, and bone marrow from one tibia and femur was prepared for flow cytometric analysis. **(A)** Gating strategy and representative gating of WT, *Il33*$^{-/-}$, and *St2*$^{-/-}$ ILC2Ps. ILC2Ps were defined as viable CD45^{+} FSC-A^{lo} SSC-A^{lo} Lin^{-} IL-25R^{+} CD25^{+} CD127^{+} cells. **(B)** The total number of viable bone marrow cells. **(C)** ILC2P frequency among live bone marrow cells. **(D)** The total number of ILC2Ps in the bone marrow. **(E)** The total number of ILC2Ps in the bone marrow of WT C57BL/6 and *Il33*$^{-/-}$ mice on a C57BL/6 background. Data are representative of three independent experiments (A) or combined from two (E, n = 8–9) or three (B-D, n = 10–13) independent experiments and displayed as the mean ± SEM. **, $P < 0.01$; ***, $P < 0.001$ by one-way ANOVA with Bonferroni posttest (B–D) or unpaired t test (E); n.s., not significant. Values within flow plots indicate percent of the parent population.

no difference was observed in the proliferation between WT and *Il33*$^{-/-}$ ILC2Ps in response to IL-33. Similarly, the proliferation index was identical between WT and *Il33*$^{-/-}$ ILC2Ps (Fig. 3 B). Finally, we counted the number of cells in each well after 5 d of culture (Fig. 3 C). IL-33 in combination with IL-2 induced a significant increase in the total number of WT and *Il33*$^{-/-}$ ILC2Ps compared with IL-2 alone. However, no difference was observed in the number of ILC2Ps between IL-33–stimulated WT and *Il33*$^{-/-}$ cultures.

We also collected supernatants from these ILC2P cultures to assess the cytokine-expressing capacity of WT and *Il33*$^{-/-}$ ILC2Ps. IL-2 alone did not induce IL-5 or IL-13 production from either WT or *Il33*$^{-/-}$ ILC2Ps. Stimulation with IL-2 and IL-33 in combination significantly induced IL-5 and IL-13 expression in both strains of ILC2Ps. A slight (∼10%) but reproducible difference in IL-5 expression was detected, with WT ILC2Ps producing marginally higher quantities of IL-5 than *Il33*$^{-/-}$ ILC2Ps (Fig. 3 D). No significant difference was observed in the expression of IL-13 between WT and *Il33*$^{-/-}$ ILC2Ps (Fig. 3 E). Collectively, these data indicate that ILC2Ps that develop in the absence of IL-33 signaling are functionally similar to WT ILC2Ps in their capacity to proliferate and express IL-5 and IL-13.

Lack of IL-33 signaling does not alter the rate of de novo ILC2P generation in the bone marrow

We also considered whether the difference in ILC2P numbers in the bone marrow of mice competent for or lacking IL-33 signaling could be explained by a different rate of generation of these cells from precursors. First, we looked at the abundance of upstream progenitor cells, specifically lymphoid-primed multipotent progenitors (LMPPs), CLPs, common helper innate lymphoid progenitors (CHILPs), and innate lymphoid cell progenitors (ILCPs), in the bone marrow of WT and *St2*$^{-/-}$ mice (gating strategy detailed in Fig. S3 and Table S3). LMPPs and CLPs can differentiate into T, B, NK, and all ILCs with varying efficiencies (Ghaedi et al., 2016). CHILPs are restricted to differentiate into ILC1s, ILC2s, and ILC3s as well as lymphoid tissue inducer cells (Klose et al., 2014). ILCPs only differentiate into ILC1s, ILC2s, and ILC3s (Constantinides et al., 2014). We did not observe any significant differences in the total number of LMPP, CLP, CHILP, or ILCP populations between WT and *St2*$^{-/-}$ mice (Fig. 3, F–I). Therefore, the first divergence in cell frequency in the ILC2 developmental lineage that we observed occurred at the mature ILC2P stage.

To assess the rate of ILC2P lymphopoiesis, we injected WT and *St2*$^{-/-}$ mice daily with BrdU for 5 d and harvested their bone marrow 24 h after the final injection to evaluate for BrdU incorporation in ILC2Ps (Fig. 3 J). BrdU incorporation is a property of lymphopoiesis and marks de novo generated cells in the bone marrow, allowing us to assess the rate of ILC2P development. A small fraction of BrdU^{+} ILC2Ps was measured in both WT and *St2*$^{-/-}$ mice. However, no significant difference in the number of BrdU^{+} ILC2Ps was observed (Fig. 3 K). Because the 5-d time course may capture

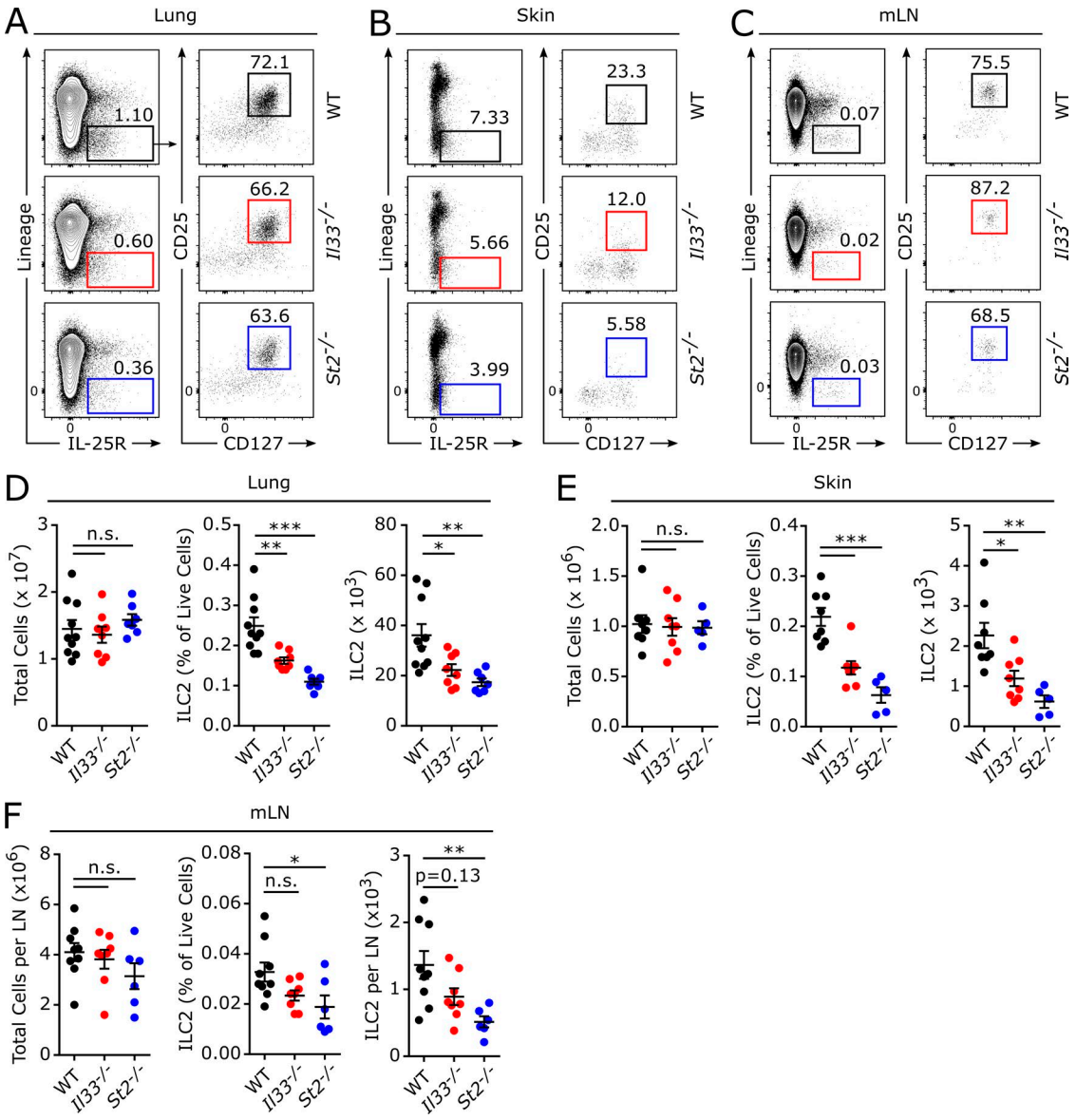

Figure 2. **Deficiency in IL-33 signaling decreases the number of ILC2s in peripheral tissues. (A–C)** Adult naive WT, *Il33*$^{-/-}$, or *St2*$^{-/-}$ mice were killed, and lungs, skin, and mLNs were collected. ILC2 representative gating in the lungs (A), skin (B), and mLNs (C). **(D)** The total number of viable lung cells (left and right lung combined), ILC2 frequency among live lung cells, and the total number of lung ILC2s. **(E)** The total number of viable skin cells (left and right ears combined), ILC2 frequency among live skin cells, and the total number of skin ILC2s. **(F)** The total number of viable mLN cells per node, ILC2 frequency among live mLN cells, and the total number of mLN ILC2s per node. Data are representative of two independent experiments (A–C) or combined from two independent experiments (D, $n = 7–10$; E, $n = 5–8$; F, $n = 6–9$) and displayed as the mean ± SEM. *, $P < 0.05$; **, $P < 0.01$; ***, $P < 0.001$ by one-way ANOVA with Bonferroni posttest (D–F); n.s., not significant. Values within flow plots indicate percentage of the parent population.

the balance of both cell division and cell death, we repeated this assay with a single injection of BrdU and analyzed the mice 2 h later. Similar results were obtained, although the total number of BrdU$^+$ ILC2Ps was substantially lower, likely because of a low rate of ILC2 lymphopoiesis in naive adult mice (not depicted). These data suggest that ILC2Ps are being generated from precursors at a similar rate in the presence or absence of IL-33 signaling. Altogether, these data demonstrate that ILC2s develop similarly in the absence of IL-33 but are increased in the bone marrow and decreased in the periphery in the absence of IL-33 signaling, suggestive of a role for IL-33 in promoting bone marrow egress.

ST2 deficiency promotes bone marrow ILC2P accumulation in the perinatal period

Initial ILC2 seeding of the lungs occurs within the first 2 wk of life in an IL-33–dependent manner, suggesting a potentially critical window in perinatal life for IL-33–dependent

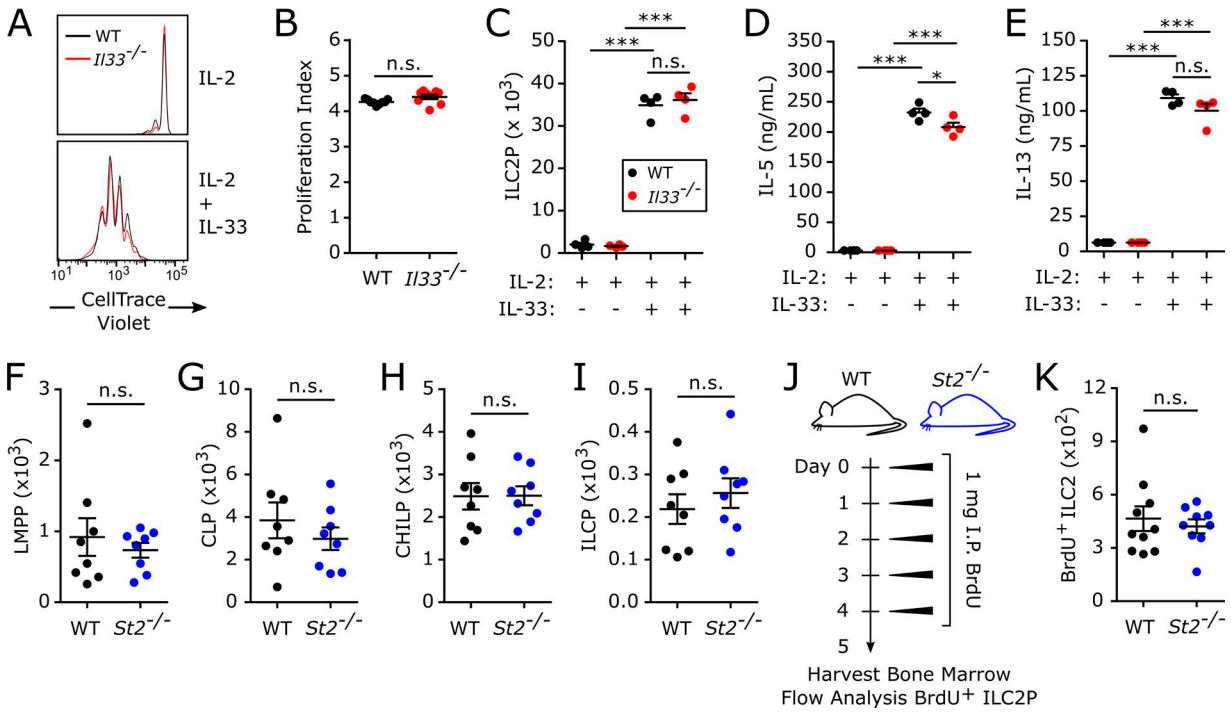

Figure 3. **WT and IL-33–deficient ILC2Ps are comparably functional and develop at a similar rate.** ILC2Ps from the bone marrow of WT and *Il33*$^{-/-}$ mice were enriched by magnetic separation and purified by FACS. Sorted ILC2Ps were stained with the dilution-based proliferation dye CellTrace Violet and cultured in supplemented RPMI medium in the presence of IL-2 (10 ng/ml) ± IL-33 (10 ng/ml) for 5 d. **(A)** Representative CellTrace Violet dilution peaks. **(B)** Proliferation index is a measure derived from CellTrace Violet staining for quantifying the mean number of proliferation events undergone by each ILC2P that was initially cultured. **(C)** Cell counts of ILC2Ps poststimulation. **(D and E)** IL-5 (D) and IL-13 (E) concentrations in the supernatants as measured by ELISA. Adult naive WT and *St2*$^{-/-}$ mice were killed, and bone marrow from one tibia and femur was prepared for flow cytometric analysis. **(F–I)** The total number of progenitors in the ILC2 lineage was quantified: LMPPs (F), CLPs (G), CHILPs (H), and ILCP (I). **(J)** WT and *St2*$^{-/-}$ mice were treated daily with 1 mg BrdU intraperitoneally for 5 d and harvested 24 h after the final dose. **(K)** The total number of BrdU^{+} ILC2Ps in the bone marrow from J. Data are combined from two independent experiments (B, $n = 9$; F–I, $n = 8$; K, $n = 9$–10) or representative of two similar experiments (A and C–E, $n = 4$). Data are displayed as the mean ± SEM. *, $P < 0.05$; ***, $P < 0.001$ by one-way ANOVA with Bonferroni posttest (C–E) or unpaired *t* test (B, F–I, K); n.s., not significant.

processes that affect ILC2 development and migration (de Kleer et al., 2016; Saluzzo et al., 2017; Steer et al., 2017). We measured ILC2Ps/ILC2s in the bone marrow and lungs of WT and *St2*$^{-/-}$ postnatal day 2 (P2) and P15 mice. P2 is before significant ILC2 seeding of the lungs, and P15 is immediately after peak ILC2 accumulation in the lungs. ILC2Ps/ILC2s were found at low but comparable levels in the bone marrow and lungs of P2 WT and *St2*$^{-/-}$ mice (Fig. 4, A, B, and E). However, ILC2Ps were significantly more abundant in the bone marrow of *St2*$^{-/-}$ P15 mice compared with WT mice (Fig. 4, C and F). Concurrently, we detected significantly fewer ILC2s in the lungs of *St2*$^{-/-}$ P15 mice compared with WT mice (Fig. 4, D and F). These data indicate the importance of IL-33 signaling in regulating ILC2P/ILC2 abundance in the bone marrow and lungs as early as the first 2 wk of life. Moreover, the progressive accumulation of ILC2Ps in the bone marrow in conjunction with reduced numbers of ILC2s in the lungs of *St2*$^{-/-}$ mice during the highly migratory perinatal period suggest a potentially critical role for IL-33–mediated bone marrow egress in initial tissue seeding by ILC2s.

Intravenously delivered IL-33 drives the egress of ILC2Ps from the bone marrow

Numerous human diseases including asthma and atopic dermatitis have been associated with increased IL-33 in the plasma (Miller, 2011). Moreover, ILC2 accumulation in the lungs of neonatal mice is associated with a wave of pulmonary IL-33 expression (de Kleer et al., 2016; Saluzzo et al., 2017; Steer et al., 2017). We hypothesized that increased circulating IL-33 may precipitate egress of ILC2s from the bone marrow. To assess the effect of IL-33 on bone marrow ILC2P egress, we intravenously injected recombinant murine IL-33 (rIL-33) or vehicle into WT mice and measured the number of ILC2Ps in the bone marrow 24 h later. Compared with vehicle treatment, intravenous delivery of rIL-33 significantly and robustly reduced the frequency and total number of ILC2Ps in the bone marrow (Fig. 5, A, C, and D). There was also a modest decrease in the total number of bone marrow cells, suggesting that exogenous rIL-33 may be promoting egress of other cell types (Fig. 5 B). However, analysis of major cell lineages in the bone marrow did not reveal a consistent loss of specific cell types other than ILC2Ps with rIL-33 treatment compared

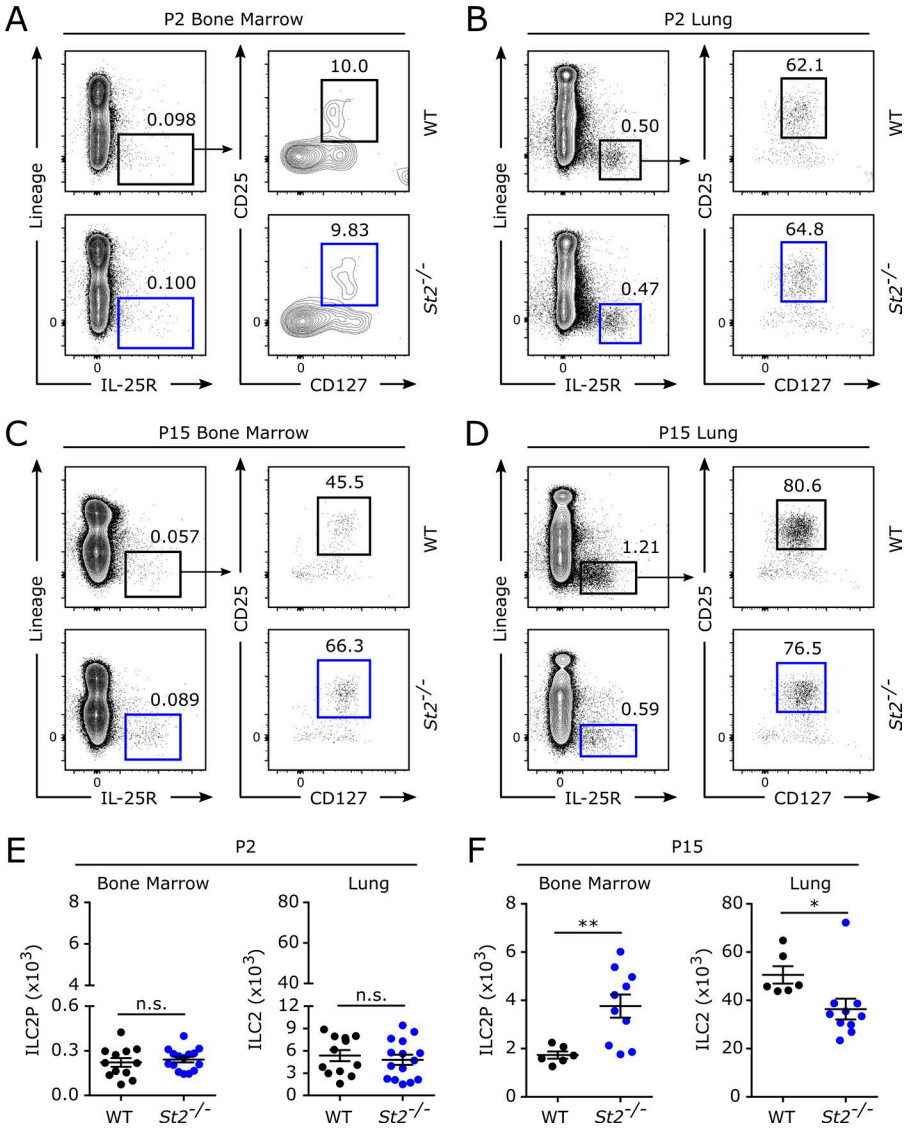

Figure 4. **IL-33 regulates ILC2/ILC2P frequencies in the bone marrow and lung of early postnatal mice.** Age-matched pups were obtained from timed breeding pairs of WT and *St2*$^{-/-}$ mice. **(A–D)** Representative gating for ILC2s and ILC2Ps in P2 bone marrow (A), P2 lungs (B), P15 bone marrow (C), and P15 lungs (D). **(E)** The total number of ILC2Ps in the bone marrow and ILC2s in the lungs of P2 mice. **(F)** The total number of ILC2Ps in the bone marrow and ILC2s in the lungs of P15 mice. Data are representative of two (C and D) or three (A and B) independent experiments or combined from two (F, n = 6–10) or three (E, n = 12–15) independent experiments and displayed as the mean ± SEM. *, P < 0.05; **, P < 0.01 by unpaired t test; n.s., not significant. Values within flow plots indicate percentage of the parent population.

with vehicle treatment (Fig. S1 D). Additionally, this IL-33–dependent egress of ILC2Ps occurred in a dose-dependent manner (Fig. 5 E). These data indicate that IL-33 is a potent inducer of ILC2P egress from the bone marrow.

ILC2P/ILC2 frequencies in *St2*$^{-/-}$ mice are established by an ILC2P/ILC2 cell-intrinsic mechanism

To dissect the mechanism responsible for IL-33–mediated ILCP2 bone marrow egress, we first determined whether the frequencies of ILC2Ps/ILC2s were established by an ILC2P/ILC2 cell-intrinsic or cell-extrinsic mechanism using a mixed bone marrow chimera model (Fig. 6 A). Whole bone marrow from BALB/c congenic WT (CD45.1$^+$) and *St2*$^{-/-}$ (CD45.2$^+$) mice was mixed in a 1:1 ratio. 10 million total cells from this mixture were transplanted into lethally irradiated WT (CD45.1$^+$ CD45.2$^+$) mice and allowed to reconstitute for 6 wk. In the bone marrow, *St2*$^{-/-}$ (CD45.2$^+$) ILC2Ps were observed at a significantly higher frequency than WT (CD45.1$^+$) ILC2Ps, consistent with our observation in germline knockout mice (Fig. 6 B). In the lungs, skin, and mLNs, WT (CD45.1$^+$) ILC2s were observed at a higher frequency than *St2*$^{-/-}$ (CD45.2$^+$) ILC2s, also consistent with our observation in germline knockout mice (Fig. 6, C–E). Next, we injected reconstituted bone marrow chimeric mice with 4 µg rIL-33 or vehicle (0.1% BSA in PBS) and evaluated the percentage reduction of ILC2Ps after 24 h. rIL-33 treatment robustly decreased the number of WT ILC2Ps in the bone marrow compared with WT ILC2Ps in vehicle-treated mice and *St2*$^{-/-}$ ILC2Ps in rIL-33–treated mice (Fig. 6 F). These data indicate that IL-33 promotes ILC2P egress in an ST2-dependent, ILC2P-intrinsic mechanism. Interestingly, rIL-33 modestly decreased *St2*$^{-/-}$ ILC2P numbers compared with vehicle treatment, suggesting that an IL-33–dependent, ILC2P-extrinsic mechanism may also contribute to ILC2P exit from the bone marrow.

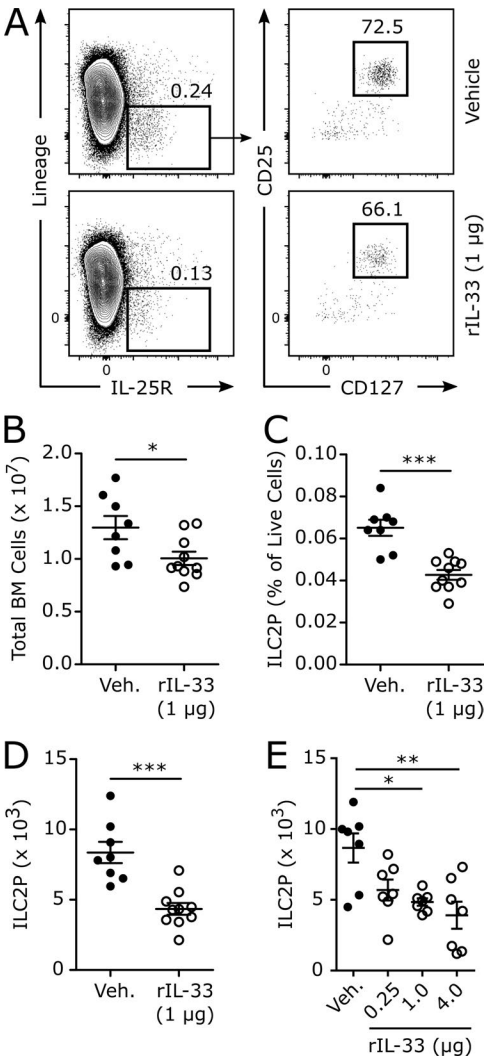

Figure 5. **Direct intravenous administration of IL-33 decreases ILC2P frequency in the bone marrow.** Adult naive WT mice were treated intravenously with rIL-33 or vehicle (0.1% BSA in PBS), and bone marrow was harvested 24 h later for flow cytometric analysis. **(A)** Representative gating for bone marrow ILC2Ps from mice treated with vehicle or 1 µg rIL-33. **(B)** The total number of viable bone marrow cells. **(C)** ILC2P frequency among live bone marrow cells. **(D)** The total number of ILC2Ps in the bone marrow. **(E)** The total number of ILC2Ps in the bone marrow of mice treated with vehicle or 0.25, 1, or 4 µg rIL-33 for 24 h. Data are combined from two independent experiments (B–D, $n = 8–10$; E, $n = 7$) or representative of two independent experiments (A) and are displayed as the mean ± SEM. *, $P < 0.05$; **, $P < 0.01$; ***, $P < 0.001$ by unpaired *t* test (B–D) or one-way ANOVA with Bonferroni posttest (E). Values within flow plots indicate percentage of the parent population.

IL-33 signaling negatively regulates CXCR4 expression to promote ILC2P exit from the bone marrow

Regulation of chemokine receptors is a cell-intrinsic mechanism by which lymphocytes guide their retention in and exit from sites of development (Griffith et al., 2014). We determined the effect of endogenous IL-33 signaling on the chemokine receptor expression pattern of bone marrow ILC2Ps. WT and *St2*$^{-/-}$ ILC2Ps were FACS-purified and screened for a panel of chemokine receptor or chemokine-associated transcripts known to be expressed by ILC2s and/or CD4^{+} Th2 cells. *St2*$^{-/-}$ ILC2Ps expressed higher levels of *Cx3cr1*, *Ccr7*, *Ccr9*, *Cxcr4*, and *Ptgdr2* and lower levels of *Ccl1* than WT ILC2Ps (Fig. 7 A). CXCR4 signaling facilitates the retention of developing leukocytes, including neutrophils and B cells in the bone marrow (Griffith et al., 2014). Therefore, we hypothesized that CXCR4 may be acting similarly to retain ILC2Ps in the bone marrow. We first confirmed our *Cxcr4* transcript analysis using *Il33*$^{-/-}$ ILC2Ps (Fig. 7 B). Next, we FACS-purified WT ILC2Ps and cultured them for 24 h with IL-2 alone or IL-2 and increasing doses of IL-33. IL-33 negatively regulated CXCR4 expression in a dose-dependent manner (Fig. 7, C and D). Moreover, IL-33 treatment of WT and *Il33*$^{-/-}$ ILC2Ps but not *St2*$^{-/-}$ ILC2Ps similarly decreased CXCR4 expression, demonstrating the ST2 specificity of IL-33–mediated CXCR4 attenuation (Fig. 7 E).

We previously demonstrated that increased circulating IL-33 promoted the egress of ILC2Ps from the bone marrow (Fig. 5). To determine whether this IL-33–mediated ILC2P egress correlated with decreased CXCR4 expression, we treated WT mice intravenously with exogenous rIL-33 (4 µg) and measured CXCR4 expression on ILC2Ps after 24 h. Compared with vehicle treatment, rIL-33 significantly decreased the expression of CXCR4 as well as the percentage of CXCR4^{+} ILC2Ps (Fig. 7 F). This effect was consistently identified with high doses of rIL-33 (4 µg) but not lower doses (1 µg, not depicted). This may be explained by egress dynamics, wherein ILC2Ps that have down-regulated CXCR4 exit the bone marrow and are no longer included in the pool of ILC2Ps that we analyzed. Higher doses of rIL-33 may induce a stronger down-regulation of CXCR4, allowing us to overcome this limitation and consistently identify differences. Alternatively, enhanced rIL-33 loads above basal levels may affect additional pathways beyond CXCR4 that influence ILC2P egress. Endogenous and exogenous IL-33 signaling did not alter CCR3 expression on other ST2^{+} populations including eosinophils, basophils, and mast cell bone marrow lineage cells and did not alter CXCR4 expression on known CXCR4^{+} cells with the exception of neutrophils, in which CXCR4 was reduced with rIL-33 treatment (Fig. S1, E and F).

To determine whether elevated CXCR4 expression in *St2*$^{-/-}$ ILC2Ps was acting to retain ILC2Ps in the bone marrow, we treated WT and *St2*$^{-/-}$ mice with AMD3100, a selective and potent antagonist of CXCR4 (Fig. 7 G). Treatment of *St2*$^{-/-}$ mice with AMD3100 significantly reduced the number of ILC2Ps in the bone marrow compared with vehicle-treated *St2*$^{-/-}$ mice (Fig. 7 H). This decrease accounted for approximately half of the difference in the number of ILC2Ps between vehicle-treated WT and *St2*$^{-/-}$ mice. AMD3100 did not significantly reduce the number of ILC2Ps in WT mice. WT ILC2Ps may be less dependent on

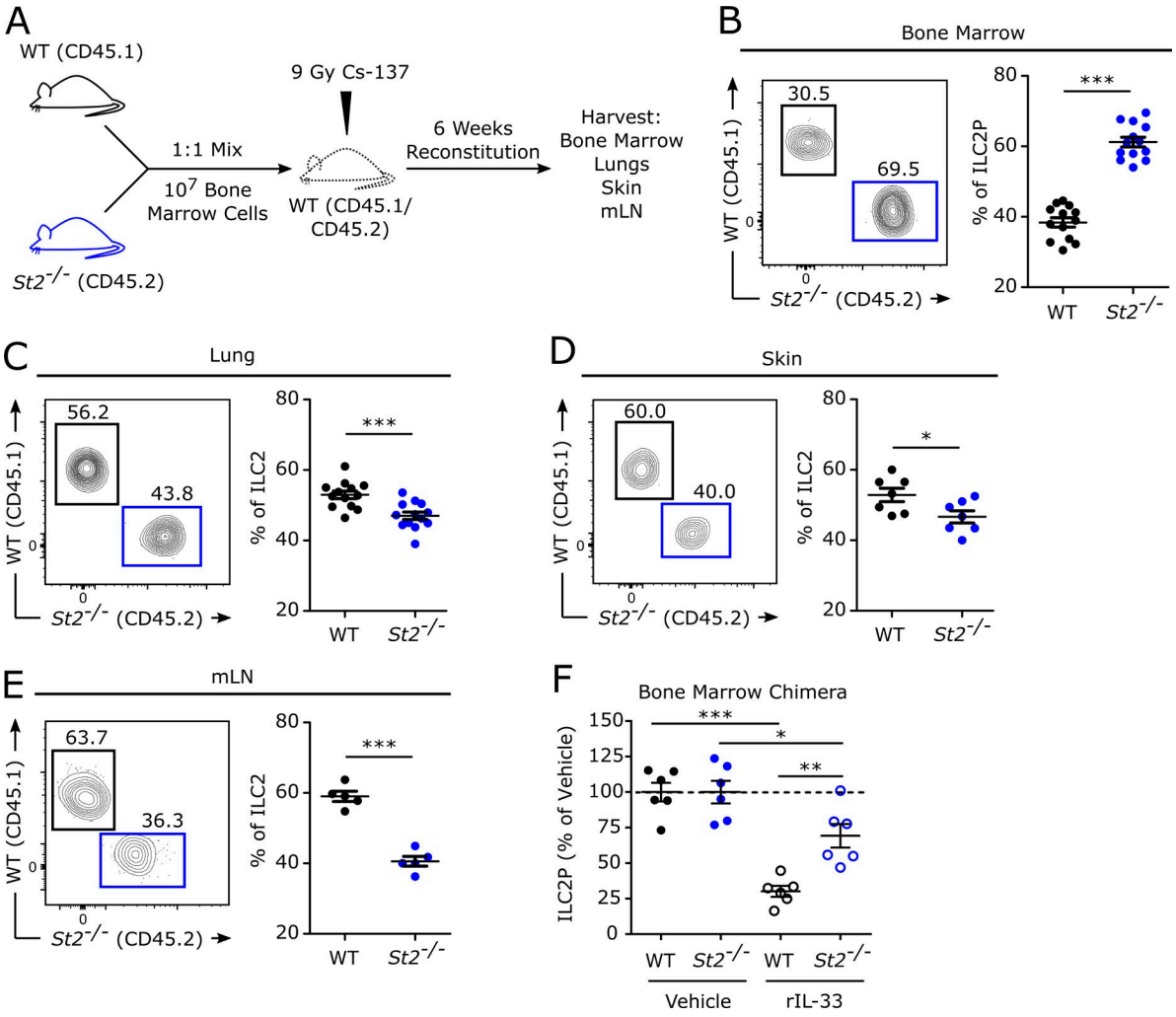

Figure 6. **Tissue frequencies of ILC2s/ILC2Ps are established by a cell-intrinsic, ST2-dependent mechanism.** 6-wk-old heterozygous CD45.1$^+$ CD45.2$^+$ WT mice were lethally irradiated and reconstituted with 10 million cells of a 1:1 mixture of CD45.1$^+$ WT and CD45.2$^+$ *St2*$^{-/-}$ total bone marrow cells. **(A)** Experimental design. **(B)** ILC2P representative gating and pooled analyses of WT and *St2*$^{-/-}$-derived ILC2Ps displayed as frequencies of donor-derived ILC2Ps. **(C–E)** ILC2 representative gating and pooled analyses of WT and *St2*$^{-/-}$-derived ILC2s displayed as frequencies of donor-derived ILC2s in the lungs (C), skin (D), and mLNs (E). **(F)** Bone marrow chimeric mice were treated intravenously with 4 µg rIL-33 or vehicle (0.1% BSA in PBS), and cells were harvested 24 h later. ILC2P total cell numbers in the vehicle-treated mice are normalized to 100% for each genotype (WT or *St2*$^{-/-}$). ILC2Ps in the rIL-33–treated mice are displayed as the percentage of vehicle-treated mice within their respective genotype. Data are combined from two (D, $n = 7$; E, $n = 5$; F, $n = 6$) or three (B and C, $n = 13$) independent experiments and displayed as the mean ± SEM. *, $P < 0.05$; **, $P < 0.01$; ***, $P < 0.001$ by unpaired *t* test (B–E) or one-way ANOVA with Bonferroni posttest (F). Values within flow plots indicate percentage of the parent population.

CXCR4 signaling for bone marrow retention considering their lower level of *Cxcr4* expression (Fig. 7, A and B). Therefore, short-course inhibition of CXCR4 with AMD3100 in WT mice may be insufficient to induce a difference in the bone marrow retention of ILC2Ps. Collectively, these data suggest that endogenous IL-33 signaling attenuates CXCR4 expression on ILC2Ps, allowing for their efficient egress from the bone marrow. Furthermore, inhibition of CXCR4 significantly, but only partially, reduced the number of ILC2Ps in the bone marrow, highlighting that IL-33 is likely regulating multiple pathways that may collaborate to promote egress.

We next considered whether CXCR4 signaling was regulating ILC2P exit from the bone marrow in early postnatal mice. ILC2Ps from P2 WT and *St2*$^{-/-}$ mice, representing a time point before significant ILC2 migration, had comparable expression of CXCR4 and a similar frequency of CXCR4$^+$ ILC2Ps (Fig. 7 I). By P15, representing a time point immediately after ILC2 migration, *St2*$^{-/-}$ ILC2Ps displayed significantly increased expression of CXCR4 compared with WT ILC2Ps (Fig. 7 J). Similarly, there was an increased frequency of CXCR4$^+$ ILC2Ps in P15 *St2*$^{-/-}$ mice compared with WT mice (Fig. 7 J). We validated these results in P15 *Il33*$^{-/-}$

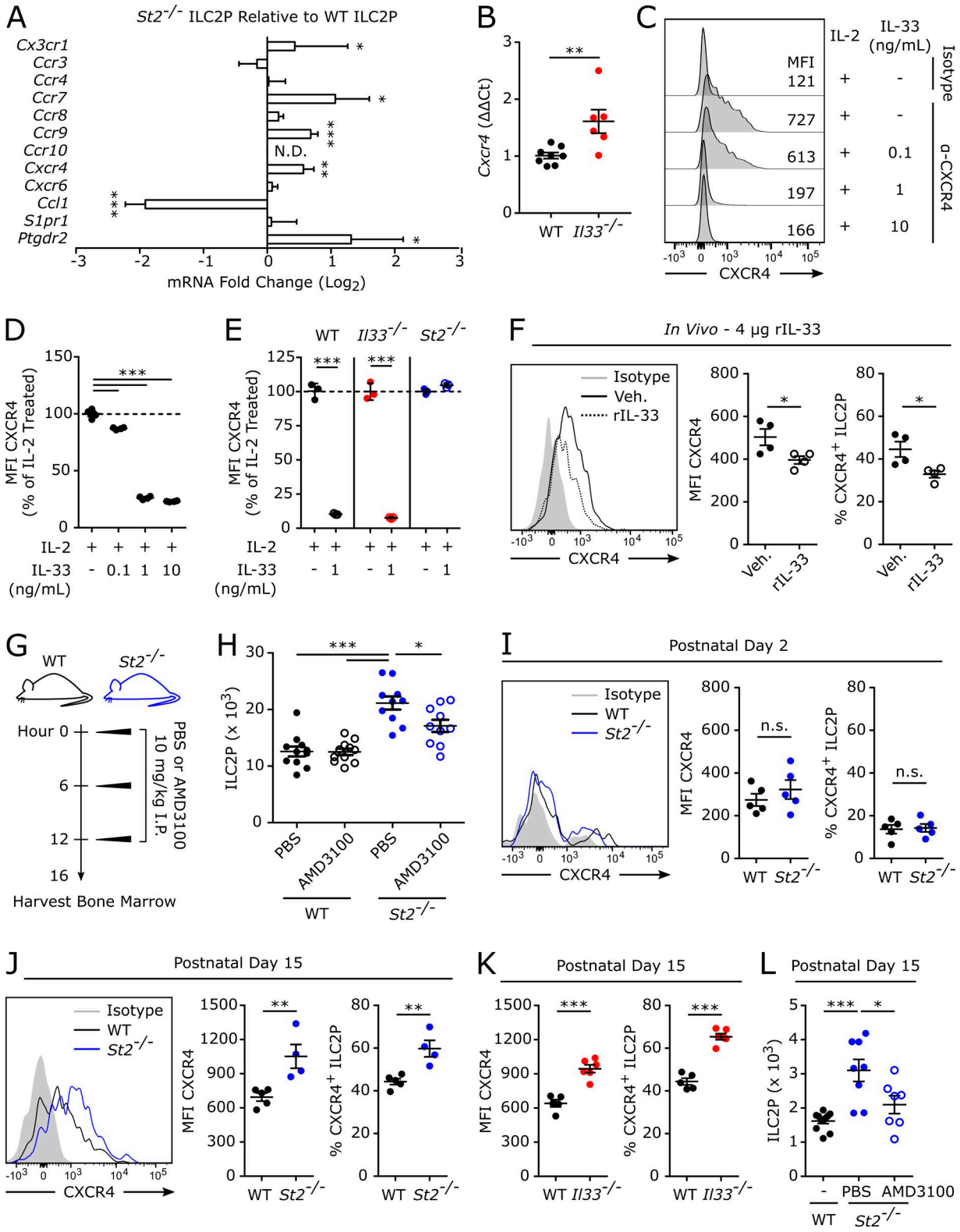

Figure 7. **IL-33 negatively regulates CXCR4 to promote efficient egress of ILC2Ps. (A)** ILC2Ps were magnetically enriched and FACS-purified from the bone marrow of WT and *St2*$^{-/-}$ mice for quantitative RT-PCR of chemokine receptors and signals. Data were normalized to a pooled set of three housekeeping genes, and differential expression was assessed by the ΔΔCt method. Data are shown as the expression level in *St2*$^{-/-}$ ILC2Ps compared with WT ILC2Ps and are displayed as a $\log_2$ fold change. **(B)** *Cxcr4* expression by quantitative RT-PCR in purified ILC2Ps from WT and *Il33*$^{-/-}$ mice. **(C)** Purified

mice (Fig. 7 K). To test whether this elevated expression of CXCR4 was responsible for ILC2P retention in early postnatal mice, we treated P15 mice with AMD3100 and evaluated the number of ILC2Ps in the bone marrow. Compared with vehicle-treated P15 *St2*$^{-/-}$ mice, AMD3100 treatment significantly reduced the number of ILC2Ps in the bone marrow (Fig. 7 L). Collectively, these data suggest that endogenous IL-33 signaling critically promotes ILC2P egress from the bone marrow by attenuating CXCR4 in the early postnatal window when ILC2s are robustly seeding tissues.

Allergic airway inflammation induced by the fungal allergen *Alternaria alternata* drives the egress of ILC2Ps from the bone marrow

Given that exogenous rIL-33 treatment mobilized ILC2s to egress from the bone marrow (Fig. 5), we sought to determine whether exposure to the fungal aeroallergen *A. alternata*, which induces significant IL-33–dependent allergic inflammation, stimulates the egress of ILC2Ps from the bone marrow. *A. alternata* is a fungal species that is associated with significant asthma morbidity in humans and drives allergic airway inflammation in mice (Salo et al., 2006; Bartemes et al., 2012; Doherty et al., 2013; Zhou et al., 2016). We challenged mice intranasally with *Alternaria* extract or vehicle for four consecutive days and harvested organs 24 h later (Fig. 8 A). We identified a significant accumulation of ILC2s and their associated cytokine products IL-5 and IL-13 in the lungs of *Alternaria* extract–challenged mice compared with vehicle-challenged mice (Fig. S4), consistent with prior research (Bartemes et al., 2012; Doherty et al., 2013; Zhou et al., 2016). Intranasal challenge with *Alternaria* extract significantly altered the cellular composition of the bone marrow, with a strong trend toward a decrease in total bone marrow cell number driven largely by a statistically significant decrease in the number of FSC-A^{lo} SSC-A^{lo} cells (Fig. 8, B–D). Among these lymphocytes, there was a statistically significant decline in the frequency and total number of ILC2Ps in the bone marrow of mice challenged with *Alternaria* extract compared with vehicle (Fig. 8, B, E, and F). Concurrently, intranasal *Alternaria* extract challenge stimulated an increase in serum IL-33 concentrations compared with vehicle (Fig. 8 G). *Alternaria* extract challenge induced significant changes in the bone marrow cellular composition in an IL-33–independent manner, with a significant decrease in FSC-A^{lo} SSC-A^{lo} cells in both WT and *St2*$^{-/-}$ mice (Fig. 8 H). However, ILC2P-specific egress required IL-33, with *Alternaria* extract challenge decreasing the number of ILC2Ps in the bone marrow of WT but not *St2*$^{-/-}$ mice (Fig. 8 I). We did not detect differences in CXCR4 expression with 4- or 10-d *Alternaria* extract challenge, or with a single 25-µg challenge of *Alternaria* extract (not depicted). These results likely reflect the dynamic challenge of capturing a down-regulation of CXCR4 expression as ILC2Ps exit the bone marrow. They may also suggest that IL-33–dependent, non-CXCR4 pathways are more critical for regulating ILC2P egress in this aeroallergen model. Beyond ILC2Ps, *Alternaria* extract challenge increased the total number of eosinophil progenitors, mast cell progenitors, and neutrophils while reducing the total number of B cells and NK cells in the bone marrow (Fig. S1 G). Collectively, these data demonstrate that allergic airway inflammation promotes egress of ILC2Ps from the bone marrow in an IL-33–dependent manner.

Tissue disruption and IL-33 promote ILC2 trafficking and tissue seeding

ILC2s are principally tissue-resident cells in adult, naive mice (Gasteiger et al., 2015; O'Sullivan et al., 2016). However, prolonged (15-d) infection with the helminth *N. brasiliensis* leads to infiltration of hematogenously sourced ILC2s (Gasteiger et al., 2015). Moreover, initial ILC2 accumulation in the lungs progresses rapidly within the first 2 wk after birth in an IL-33–dependent manner (de Kleer et al., 2016; Saluzzo et al., 2017; Steer et al., 2017). Using a parabiosis model with sublethal radiation exposure, we sought to model tissue disruption and empty niche filling to determine whether IL-33 augments hematogenous trafficking of ILC2s. First, WT congenic CD45.1^{+} C57BL/6 mice were left nonirradiated or were treated with a sublethal dose (5 Gy) of radiation and subjected to parabiosis with naive WT CD45.2^{+} C57BL/6 mice (Fig. 9 A). We performed these surgeries in C57BL/6 mice, as we found that parabiosis of BALB/c mice caused significant mortality (>60% mortality by 4 wk after

ILC2Ps from WT mice were treated for 24 h in vitro with IL-2 in combination with varying doses of IL-33 and assessed for CXCR4 expression. **(D)** Quantification of C. **(E)** CXCR4 expression in purified ILC2Ps from WT, *Il33*$^{-/-}$, and *St2*$^{-/-}$ mice that were treated for 24 h in vitro with 1 ng/ml IL-33. For D and E, IL-2–treated WT, *Il33*$^{-/-}$, and *St2*$^{-/-}$ samples are normalized to 100%, and IL-33–treated samples are displayed as a percentage of IL-2–treated samples within each genotype (WT, *Il33*$^{-/-}$, and *St2*$^{-/-}$). **(F)** Mean fluorescence intensity (MFI) of CXCR4 on ILC2Ps and the percentage of ILC2Ps expressing CXCR4 in adult female mice that were treated intravenously with 4 µg rIL-33 or vehicle and killed 24 h later. **(G)** WT and *St2*$^{-/-}$ mice were treated intraperitoneally with three doses of AMD3100 (10 mg/kg) or PBS vehicle given every 6 h, and bone marrow was collected for flow cytometric analysis 4 h after the final AMD3100 dose. **(H)** Total number of ILC2Ps in the bone marrow from adult female WT and *St2*$^{-/-}$ mice treated as in G. **(I)** MFI of CXCR4 on ILC2Ps, and the percentage of ILC2Ps expressing CXCR4 in P2 WT and *St2*$^{-/-}$ mice. **(J)** MFI of CXCR4 on ILC2Ps, and the percentage of ILC2Ps expressing CXCR4 in P15 WT and *St2*$^{-/-}$ mice. **(K)** MFI of CXCR4 on ILC2Ps, and the percentage of ILC2Ps expressing CXCR4 in P15 WT and *Il33*$^{-/-}$ mice. **(L)** Total number of ILC2Ps in the bone marrow of P15 WT and *St2*$^{-/-}$ mice treated as in G. Data are combined from two (B, n = 6–8; L, n = 7–11) or three (A, n = 12; H, n = 10–11) independent experiments or are representative of two (E, n = 3; F, n = 4; I, n = 5; K, n = 5–6) or three (C and D, n = 4; J, n = 4–5) independent experiments and displayed as the mean ± SEM. *, $P < 0.05$; **, $P < 0.01$; ***, $P < 0.001$ by one-way ANOVA with Bonferroni posttest (D, H, and L) or unpaired t test (A, B, E, F, and I–K); n.s., not significant; N.D., not detected.

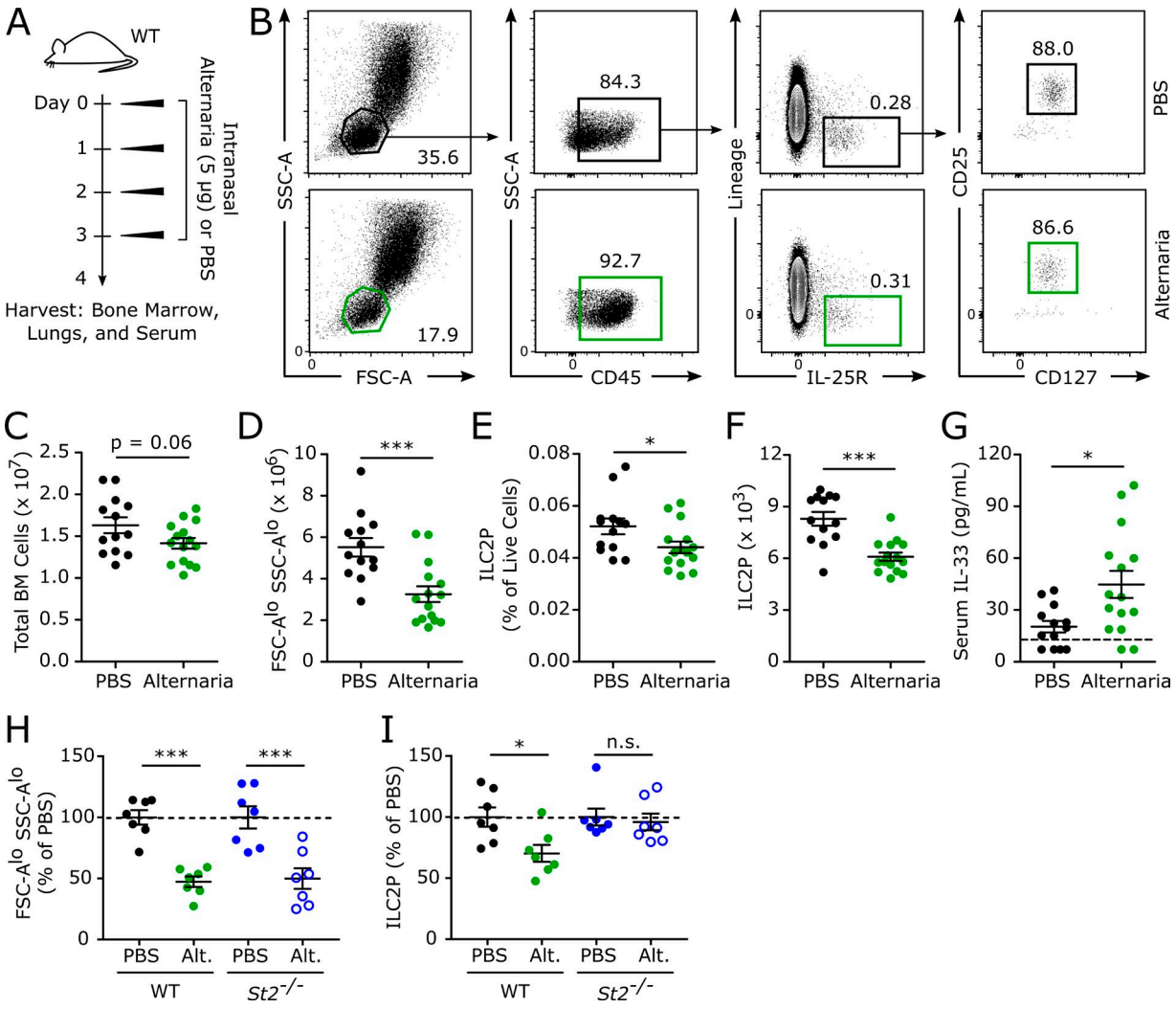

Figure 8. **Allergic airway inflammation induced by the fungal aeroallergen *A. alternata* promotes increased serum IL-33 and ILC2P egress from the bone marrow. (A)** Adult WT mice were treated for four consecutive days with an intranasal challenge of *A. alternata* extract or PBS vehicle and killed 24 h after the final treatment. **(B)** Representative gating for ILC2Ps in the bone marrow. **(C)** The total number of viable bone marrow cells. **(D)** The total number of FSC-A^{lo} SSC-A^{lo} cells in the bone marrow. **(E)** ILC2P frequency among live bone marrow cells. **(F)** The total number of ILC2Ps in the bone marrow. **(G)** The concentration of IL-33 in the serum as measured by ELISA. **(H)** The total number of FSC-A^{lo} SSC-A^{lo} cells. **(I)** ILC2Ps in WT and *St2*$^{-/-}$ mice treated for four consecutive days with *Alternaria* extract. For H and I, PBS-treated WT and *St2*$^{-/-}$ mice were normalized to 100%, and *Alternaria* extract–treated mice are displayed as a percentage of PBS-treated within each genotype (WT and *St2*$^{-/-}$). Data are combined from two (H and I, $n = 7$) or three independent experiments (C–G, $n = 13$–15) or representative of three independent experiments (B) and displayed as the mean ± SEM. *, $P < 0.05$; ***, $P < 0.001$ by unpaired *t* test (C–G) or one-way ANOVA with Bonferroni posttest (H and I); n.s., not significant. Dashed line in G indicates limit of detection of the assay. Values within flow plots indicate percentage of the parent population.

surgery, unpublished observation). Parabiotic mouse pairs were housed for 6 wk before tissues were harvested, allowing for cells to exchange hematogenously between partners. In the spleens of nonirradiated:naive mouse pairs, highly mobile populations including CD4$^+$ T cells, CD8$^+$ T cells, and B cells were identified in an ∼1:1 ratio, indicating the formation of a robust vascular bridge across the parabionts (Fig. 9 B). We next assessed for the number of trafficked CD45.2$^+$ ILC2s in the tissues from the WT congenic CD45.1$^+$ mice. In the nonirradiated mice, we found very few trafficked CD45.2$^+$ ILC2s (<5%) in the lungs, skin, or mLNs (Fig. 9, C and D), consistent with prior studies (Gasteiger et al., 2015; O'Sullivan et al., 2016). However, in the irradiated mice, we found significant increases in the percentage of trafficked CD45.2$^+$ ILC2s in the lungs, skin, and mLNs (Fig. 9, C and D). Little to no trafficking of ILC2s was observed from the CD45.1$^+$ parabionts into the CD45.2$^+$ parabionts as expected, with radiation exposure in the CD45.1$^+$ mouse further reducing basal trafficking of ILC2s to the CD45.2$^+$ mouse, possibly because of modest dysfunctions in lymphopoiesis as a result

of sublethal radiation exposure (Fig. 9 E). Collectively, these data demonstrate a critical capacity for ILC2s to traffic hematogenously to repopulate disrupted tissues.

We next sought to understand how IL-33 shapes the ability of ILC2s to traffic and reseed tissues. Sublethally irradiated WT CD45.1$^+$ mice were subjected to parabiosis with naive WT CD45.2$^+$ mice and rested for 2 wk. Mice were subsequently treated twice weekly with intravenous vehicle or rIL-33 (2 µg per parabiotic pair) for four consecutive weeks, and organs were harvested to assess for ILC2 trafficking to the lungs, skin, and mLNs (Fig. 9 F). rIL-33 treatment produced a threefold enrichment of trafficked CD45.2$^+$ ILC2s in the lungs of CD45.1$^+$ mice compared with vehicle treatment (Fig. 9, G and H). However, IL-33 did not significantly affect ILC2 migration from the naive mouse to the skin or mLNs of the irradiated parabiont in this model. Moreover, CD45.1$^+$ ILC2s did not substantially infiltrate the CD45.2$^+$ tissues with or without rIL-33 treatment (Fig. 9 I). Thus, IL-33 critically enhances ILC2 hematogenous migration and tissue repopulation in a lung-tropic manner. These results demonstrate the potential importance of IL-33–associated mechanisms, such as promoting bone marrow egress, that mobilize ILC2s for hematogenous spread.

DISCUSSION

In this study, we evaluated the effect of IL-33 on the development and egress of ILC2Ps from the bone marrow. IL-33 was a critical regulator of ILC2P egress from the bone marrow. Mice lacking IL-33 signaling accumulated ILC2Ps in the bone marrow significantly more than WT controls, and exogenous, intravenous rIL-33 treatment of mice significantly reduced the number of ILC2Ps in the bone marrow. IL-33–mediated egress was critically important in the perinatal period, when ILC2s are rapidly populating tissues. ILC2P egress occurred in an ILC2P-intrinsic, IL-33–dependent manner, with IL-33 negatively regulating the bone marrow retentive chemokine receptor CXCR4. Fungal aeroallergen challenge with *Alternaria* extract promoted ILC2P egress in an IL-33–dependent manner. Finally, IL-33 augmented ILC2 hematogenous trafficking to the lungs in a parabiosis model of tissue disruption and repopulation. Collectively, these data establish a novel role for IL-33 in promoting the egress of ILC2Ps from the bone marrow.

Several prior studies have identified modest to significant reductions in the number of ILC2s in peripheral tissues of naive or vehicle-treated mice in the absence of IL-33 signaling, especially in the perinatal period (Bartemes et al., 2012; Hardman et al., 2013; Li et al., 2014; Brestoff et al., 2015; de Kleer et al., 2016; Saluzzo et al., 2017; Steer et al., 2017). We had initially hypothesized that this may be caused by a developmental impedance, as IL-33 promotes ILC2 differentiation from CLPs in vitro (Wong et al., 2012; Xu et al., 2015). Surprisingly, IL-33 appeared dispensable for the development of ILC2Ps that are able to proliferate and produce IL-5 and IL-13. Further characterization of ILC2 development will be necessary to assess whether ILC2 functions beyond proliferative potential, and IL-5/IL-13 producing capacity may be affected by development in an IL-33–deficient environment.

Our data do point to a vital role for IL-33 in promoting efficient egress of ILC2Ps from the bone marrow, at least partially via direct signaling on ILC2Ps to negatively regulate CXCR4. Our results suggest that this IL-33/CXCR4 effect is most pronounced in the perinatal period when ILC2s are rapidly seeding tissues, as differences in CXCR4 expression and inhibition via AMD3100 were most evident in P15 mice compared with adult mice. However, exogenous IL-33 exposure still mobilized ILC2P egress in adult mice. Therefore, additional IL-33–dependent pathways may collaborate with CXCR4 to promote retention or egress of ILC2Ps, particularly in adult mice. In neutrophils and hematopoietic stem cells, CXCR4 works in conjunction with the integrin VLA-4 to mediate retention in the bone marrow (Bonig et al., 2009; Petty et al., 2009). It is intriguing to consider VLA-4/VCAM-1 as a potential collaborator, but further work will be needed to establish a role for integrins in ILC2P bone marrow retention. In addition, in vivo CXCR4 inhibition with AMD3100 is not specific to ILC2Ps, and therefore we cannot at the present time definitively exclude an indirect mechanism of action for CXCR4 blockade in promoting ILC2P bone marrow egress. Warts, hypogammaglobulinemia, immunodeficiency, and myelokathexis (WHIM) syndrome is a rare autosomal dominant disorder in which mutations in CXCR4 lead to hyperactive or prolonged signaling through this receptor (Kawai and Malech, 2009). Patients with WHIM syndrome present with recurrent infections, hypogammaglobulinemia, and retention of neutrophils in the bone marrow. WHIM syndrome may represent a clinical scenario in which we can better understand the role of CXCR4 signaling in human ILC2 biology.

The extent and timing of ILC trafficking remains an area of ongoing investigation. Early work performed in naive, adult parabiotic mice demonstrated that in the unchallenged setting, ILCs including ILC2s are predominantly tissue resident (Gasteiger et al., 2015; O'Sullivan et al., 2016). However, protracted type 2 inflammation associated with *N. brasiliensis* infection induced moderate infiltration of ILC2s but not ILC1s or ILC3s to the sites of inflammation (Gasteiger et al., 2015). Short-term intranasal delivery of IL-33 did not elicit significant ILC2 trafficking to the lungs in parabiotic mice (Moro et al., 2016), but extended allergen exposure correlated with increased ILC2s in the blood and accumulation of ILC2s in the lungs in a β_2 integrin–dependent manner that was independent of proliferation or apoptosis, suggestive of trafficking (Karta et al., 2017). Further evidence for trafficking of ILCs was obtained using the Kaede transgenic mouse model in which inducible photoconverted ILCs were tracked from the intestinal tissue to draining lymph nodes in significant quantities (Mackley et al., 2015). Several important differences in the design of these experiments may explain the divergent results. Specif-

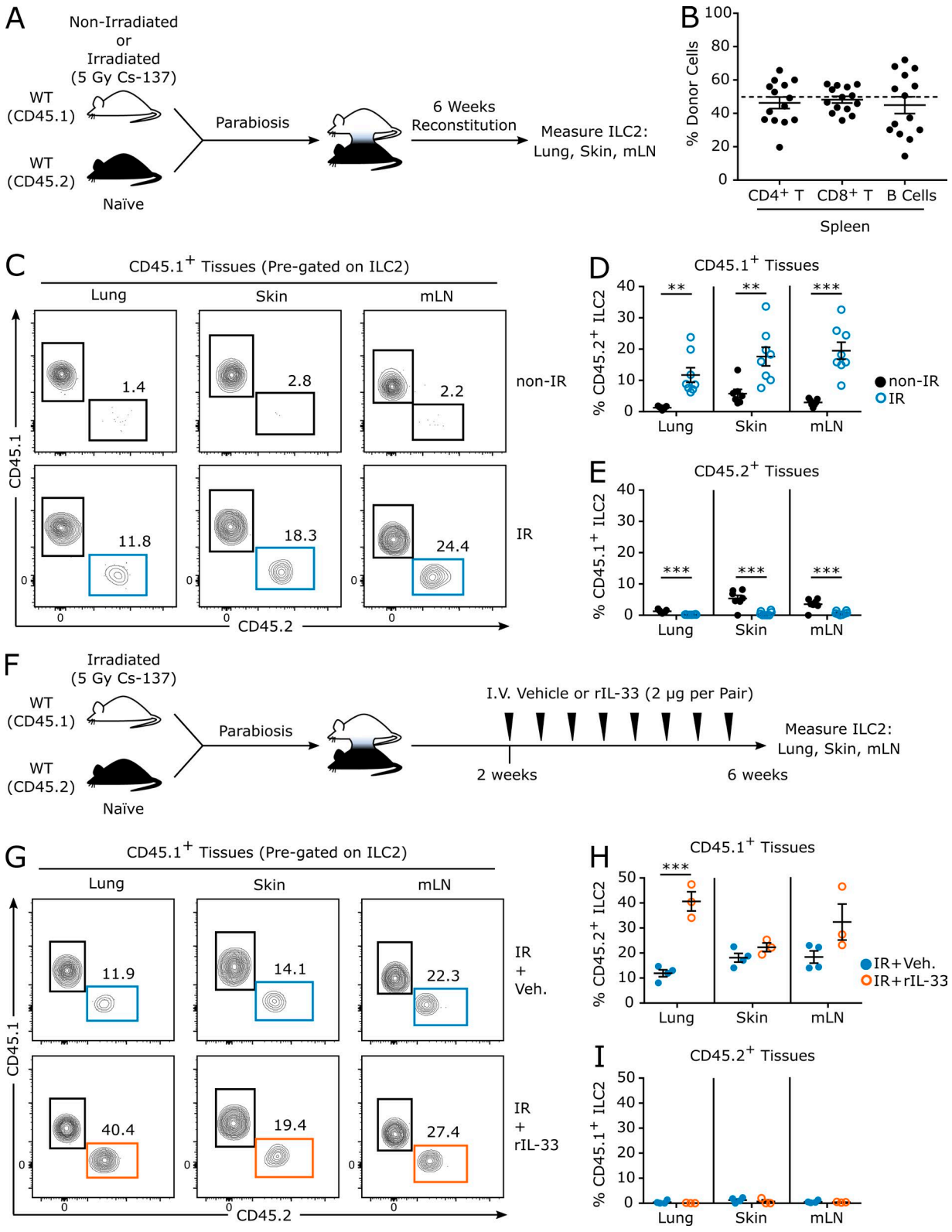

Figure 9. **IL-33 and tissue disruption promote ILC2 trafficking for tissue repopulation. (A)** Experimental design for B–E: C57BL/6 congenic CD45.1+ WT mice were either irradiated with 5 Gy or not irradiated, and were subjected to parabiosis with naive C57BL/6 CD45.2+ WT mice for 6 wk. **(B)** Percentage of donor CD4+ T, CD8+ T, and B cells in recipient tissues from nonirradiated mouse pairs. **(C)** Representative flow plots. **(D)** Quantification of the frequency of CD45.2+ ILC2s collected from the lung, skin, and mLNs of the CD45.1+ parabiont (irradiated or nonirradiated). **(E)** Quantification of the frequency of CD45.1+

ically, the length of the tissue disruption, the strength of the tissue inflammatory stimulus, and the quality of the associated inflammation (type 1 vs. type 2) are all likely factors in influencing the degree of ILC2 trafficking. Together, these data suggest that although ILC2s are primarily tissue resident, reseeding may occur in the appropriate inflammatory setting such as infection and allergen challenge.

In our study, we used a parabiotic model of radiation-induced tissue disruption to create an empty-niche effect. Our principal aim was to study ILC2 trafficking during the population of tissues, with implications for initial ILC2 seeding of tissues during development and the repopulation of ILC2s after substantial tissue disruption. Our data demonstrate that radiation-induced tissue disruption elicited marked reseeding of the lungs, skin, and mLNs by hematogenously sourced ILC2s. Moreover, intravenous IL-33 treatment significantly increased ILC2 trafficking to the lungs in this model. Radiation induced a similar tissue-migratory effect in human severe combined immunodeficiency patients receiving hematopoietic stem cell transplants for tissue reseeding with donor ILC2s (Vély et al., 2016). Together, our data in conjunction with published research support a participatory role for ILC2 trafficking, augmented by IL-33, during initial tissue seeding and in settings of repopulation after depletion of resident ILC2s.

Increased plasma concentrations of IL-33 have been observed in numerous human diseases including asthma (Bonanno et al., 2014; Bahrami Mahneh et al., 2015; Chauhan et al., 2015), atopic dermatitis (Tamagawa-Mineoka et al., 2014), allergic rhinitis (Glück et al., 2012), inflammatory bowel disease (Pastorelli et al., 2010; Saadah et al., 2015), rheumatoid arthritis (Matsuyama et al., 2010; Mu et al., 2010), and psoriasis (Mitsui et al., 2016), among others. In many of these diseases, ILC2s are thought to participate in driving inflammation. Our data in mice demonstrate that the intravenous delivery of rIL-33 mobilizes ILC2Ps to egress from the bone marrow. Moreover, fungal aeroallergen challenge in mice promoted the exit of ILC2Ps from the bone marrow in an IL-33–dependent manner. It is interesting to consider whether a similar effect exists in humans, and whether anti-IL-33 therapeutics currently in development may reduce inflammation by not only blocking local tissue effects but also reducing the recruitment of new ILC2s. Although some evidence suggests that ILC2s may traffic with strong, protracted type 2 inflammatory stimuli (Gasteiger et al., 2015; Karta et al., 2017), further studies will be necessary to understand the possible migration of ILC2s during allergic inflammation, as our trafficking studies primarily focused on a model of empty niche filling rather than allergic inflammation.

IL-33 regulated the expression of multiple chemokine receptors in ILC2Ps. Specifically, IL-33 decreased the expression of *Cx3cr1*, *Ccr7*, *Ccr9*, *Cxcr4*, and *Ptgdr2* and increased the expression of *Ccl1*. Notably, CCR9 is a gut-tropic signaling pathway (Griffith et al., 2014), and IL-33 may be skewing ILC2 migration toward sites outside of the gastrointestinal tract. Within the gastrointestinal tract, tuft cell–derived IL-25 is thought to be a key regulator of ILC2 responsiveness (Howitt et al., 2016; von Moltke et al., 2016). Tuft cells are not major sources of IL-33, and any trafficking bias induced by IL-33 may function to guide cells to areas of higher IL-33 content. rIL-33 treatment preferentially guided ILC2s to the lungs in our parabiosis model, consistent with this hypothesis.

Given the effect of IL-33 on regulating chemokine receptor expression in bone marrow ILC2Ps, it is plausible that IL-33 may also shape the chemokine receptor profiles of peripheral ILC2s. Beyond retention of cells in the bone marrow, CXCR4 is involved in several biological processes including the trafficking of lymphocytes into secondary lymphoid organs (Griffith et al., 2014). ILC2s readily cycle between tissues and adjacent lymph nodes (Mackley et al., 2015) and also interface with the adaptive immune system (Moro et al., 2010; Drake et al., 2014, 2016; Gold et al., 2014; Halim et al., 2014, 2016; Mirchandani et al., 2014; Oliphant et al., 2014). Whether peripherally expressed IL-33 affects ILC2 trafficking between tissues and secondary lymphoid organs in a CXCR4-dependent manner remains unknown. IL-33 may also work in combination with other signals to exert tissue-specific effects on ILC2 chemokine receptor expression, and additional characterization will be needed on a tissue-by-tissue basis.

Herein, our data provide evidence that IL-33 promotes the egress of ILC2Ps from the bone marrow. Mice lacking IL-33 signaling had a significant accumulation of ILC2Ps in the bone marrow, including during the critical perinatal period associated with ILC2 accumulation in tissues, that was mechanistically driven by an overexpression of CXCR4. Intravenously delivered IL-33 and fungal allergen challenge rapidly and significantly mobilized ILC2Ps to egress from the bone marrow. These data broadly expand our understanding of IL-33 biology and ILC2 migration.

ILC2s collected from the lung, skin, and mLNs of the CD45.2$^+$ parabiont. **(F)** Experimental design for G–I: C57BL/6 congenic CD45.1$^+$ WT mice were irradiated with 5 Gy and subjected to parabiosis with naive C57BL/6 CD45.2$^+$ WT mice. 2 wk after surgery, mouse pairs were treated intravenously twice weekly with vehicle (0.1% BSA in PBS) or 2 µg rIL-33 for four consecutive weeks. **(G)** Representative flow plots. **(H)** Quantification of the frequency of CD45.2$^+$ ILC2s collected from the lung, skin, and mLNs of the CD45.1$^+$ parabiont. **(I)** Quantification of the frequency of CD45.1$^+$ ILC2s collected from the lung, skin, and mLNs of the CD45.2$^+$ parabiont. Data are combined from two (B, $n = 14$; D and E, $n = 7–8$; H and I, $n = 3–4$) independent experiments or representative of two (C and G) independent experiments and displayed as the mean ± SEM. **, $P < 0.01$; ***, $P < 0.001$ by unpaired t test. Values within flow plots indicate percentage of the parent population.

MATERIALS AND METHODS

Mice

Female 8–12-wk-old *Il33*$^{-/-}$, *St2*$^{-/-}$, and *Tslpr*$^{-/-}$ mice on a BALB/c genetic background were used throughout this article, unless otherwise indicated, and were generated as previously described (Townsend et al., 2000; Carpino et al., 2004; Zhou et al., 2005; Hardman et al., 2013). WT BALB/c mice were obtained from the Jackson Laboratory and used as controls. In some experiments, BALB/c congenic CD45.1$^+$ WT (CByJ.SJL(B6)-Ptprc^a/J) mice were obtained from the Jackson Laboratory and used as controls. Where indicated, experiments were performed with C57BL/6 mice. C57BL/6 WT and C57BL/6 congenic CD45.1$^+$ WT (B6.SJL-Ptprc^{a}Pepc^b/BoyJ) mice were obtained from the Jackson Laboratory, and *Il33*$^{-/-}$ mice on a C57BL/6 background were generated as previously described (Oboki et al., 2010). Heterozygous BALB/c CD45.1$^+$ CD45.2$^+$ WT mice were generated from crossing BALB/c mice with CByJ.SJL(B6)-Ptprc^a/J mice. Age-matched pups were obtained from timed breeding of BALB/c WT, *Il33*$^{-/-}$, and *St2*$^{-/-}$ mice. All animals were used in compliance with the revised 1996 Guide for the Care and Use of Laboratory Animals prepared by the Committee on Care and Use of Laboratory Animals of the Institute of Laboratory Animal Resources, National Research Council. All animal experiments were approved by the Vanderbilt Institutional Animal Care and Use Committee. Animals were housed under specific pathogen–free conditions. Animals were anesthetized with ketamine/xylazine and killed with pentobarbital overdose.

Flow cytometry

Bone marrow was isolated by flushing the tibia and femur with cold RPMI medium. For mLNs and spleen, tissue was grated through a 70-µm strainer into cold RPMI medium. The external portions of the left and right ears were collected for evaluation of skin ILC2s. For the disruption of the lungs and skin, tissue was mechanically minced and digested with 1 mg/ml collagenase (C5138; Sigma-Aldrich) and 0.02 mg/ml DNase I (D4527; Sigma-Aldrich) in RPMI with 5% FBS for 55 min at 37°C as previously described (Stier et al., 2016). EDTA was added to quench the enzymatic reaction, and the tissue was filtered through a 70-µm strainer. RBC lysis was performed, and all samples were counted with Trypan blue exclusion to assess total numbers of cells within each tissue. Three to five million cells were stained for flow cytometry in FACS buffer (PBS + 3% FBS). Cells were initially blocked with a 1:25 dilution of anti-CD16/CD32 blocking reagent (553142; BD Biosciences) and were subsequently stained for combinations of the surface markers listed in Table S1. Viability dye (DAPI or PI) was added immediately before flow cytometric analysis. Samples were measured on a BD LSR II and analyzed with FlowJo version X. Doublets were removed based on forward/side scatter properties, and dead cells were excluded in all analyses as PI$^+$ or DAPI$^+$. ILC2s and ILC2Ps were defined as CD45$^+$ Lin$^-$ IL-25R$^+$ CD25$^+$ CD127$^+$, where Lin represents a lineage cocktail containing antibodies against CD3, CD5, CD45R (B220), CD11b, Gr-1 (Ly-6G/C), 7-4, and Ter-119. ILC2s and ILC2Ps defined by this gating strategy coexpressed validated phenotypic markers found on ILC2s in a variety of tissues in WT mice including CD90, ST2, and ICOS, although ST2 expression was not observed in the skin (Fig. S5). In some experiments, cells were stained for donor source using anti-CD45.1 or anti-CD45.2 (Table S1). Full gating strategies for all cell types assessed throughout the article are listed in Table S3.

In vitro ILC2P culture

Bone marrow was prepared as described in Flow cytometry. After RBC lysis, samples were enriched for Lin-negative cells by magnetic separation per manufacturer instructions (130-110-470; Miltenyi Biotec). Enriched cell fractions were prepared for FACS, and ILC2Ps were sorted on a BD FACSAria III into RPMI with 10% FBS, 2 mM L-glutamine, 1 mM sodium pyruvate, 10 mM Hepes, and 100 units/ml penicillin and streptomycin. In some assays, ILC2Ps were stained before culture with the dilution-based proliferation dye CellTrace Violet per manufacturer instructions (C34557; Life Technologies). ILC2Ps were plated at 2,500 cells/well in 96-well round-bottom plates. ILC2Ps were cultured with IL-2 (10 ng/ml, 212-12; PeproTech) alone or in combination with IL-33 (0.1–10 ng/ml, 210-33; PeproTech) for 1–5 d.

Protein measurements

Cell culture supernatants from in vitro ILC2P cultures were collected for the measurement of IL-5 and IL-13 by ELISA (DY405 and DY413; R&D Systems) per manufacturer instructions. Serum IL-33 protein levels were measured by ELISA (M3300; R&D Systems) per manufacturer instructions.

BrdU assay

Mice were treated in vivo with 1 mg BrdU intraperitoneally either once and killed 2 h later or once daily for five consecutive days and killed 24 h later. Bone marrow was harvested 24 h after the final treatment, and cells were prepared for flow cytometric analysis per manufacturer instructions (552598; BD Biosciences). In brief, cells were stained with a fixable live/dead viability dye (13-0868; Tonbo Biosciences) followed by anti-CD16/CD32 blockade and antibodies against ILC2P cell-surface markers (Table S1). Cells were fixed and permeabilized, and the DNA was treated with DNase I for 1 h at 37°C to expose BrdU epitopes. Cells were subsequently stained with an anti-BrdU antibody and measured by flow cytometry to assess the total number of BrdU$^+$ ILC2Ps in the bone marrow.

Bone marrow chimeras

6- to 10-wk-old heterozygous CD45.1$^+$ CD45.2$^+$ WT BALB/c recipients were lethally irradiated (9 Gy) and transplanted with a 1:1 mixture of whole bone marrow from age-matched 6- to 10-wk-old BALB/c WT congenic (CD45.1$^+$)

and *St2*$^{-/-}$ (CD45.2^{+}) mice via retroorbital injection while anesthetized with ketamine/xylazine. Mice were provided with sulfamethoxazole/trimethoprim in the drinking water for 2 wk after transplant and were maintained in sterile housing. Bone marrow grafts were allowed to reconstitute for 6 wk. Mice were subsequently killed to collect bone marrow, lungs, skin, and mLNs to assess donor frequencies by flow cytometry. Residual cells remaining from the recipient mice (CD45.1^{+} CD45.2^{+}) were excluded.

mRNA quantification

ILC2Ps from WT, *Il33*$^{-/-}$, and *St2*$^{-/-}$ mice were enriched for Lin-negative cells by magnetic separation and purified by FACS as described in Flow cytometry. Cells were sorted into cold PBS and centrifuged at 10,000 *g* for 5 min to remove the supernatant. mRNA was collected from the pelleted ILC2Ps using the RNeasy Micro kit (74004; QIAGEN) with on-column DNase treatment. cDNA was prepared using the SuperScript IV reverse transcription system (18091050; Invitrogen). Because of low cell input (fewer than 20,000 sorted ILC2Ps per sample), we performed a preamplification for our target genes as per manufacturer instructions (4384267; Applied Biosystems). A conventional quantitative PCR using the preamplification product and FAM-MGB TaqMan primers listed in Table S2 was performed on an Applied Biosystems QuantStudio12k Flex Real-Time PCR machine, and data were analyzed using Applied Biosystems QuantStudio 12k Flex Software v.1.2.2. Six candidate housekeeping genes were evaluated for stable expression in ILC2Ps as previously described (Vandesompele et al., 2002), and target genes were normalized to the geometric mean Ct values of a pool of three of these stably expressed reference genes: Rpl13a, Ywhaz, and Hprt. Differential expression was assessed by using the ΔΔCt protocol.

In vivo AMD3100 and IL-33 treatments

For CXCR4 blockade, mice were treated with intraperitoneal injections of 10 mg/kg AMD3100 (A5602; Sigma-Aldrich) or vehicle PBS every 6 h for a total of three consecutive doses. Mice were killed 4 h after the final dose of AMD3100. For IL-33 treatments, mice were anesthetized with ketamine/xylazine and treated with 0.25, 1, or 4 µg rIL-33 (210-33; PeproTech) or vehicle (0.1% BSA in PBS) via retroorbital injection. Mice were killed 24 h after IL-33 injection.

In vivo challenge with *A. alternata* extract

WT and *St2*$^{-/-}$ mice were anesthetized with ketamine/xylazine and challenged intranasally with either 5 µg *A. alternata* extract (Greer) dissolved in 100 µl PBS or 100 µl PBS (vehicle) every 24 h for four consecutive days. Mice were killed 24 h after the final dose of *Alternaria* extract, and serum, lungs, and bone marrow were collected for analysis.

Parabiosis

C57BL/6 congenic CD45.1^{+} WT mice were left untreated or were sublethally irradiated (5 Gy) and parabiosed to C57BL/6 CD45.2^{+} WT mice. Mice were anesthetized with ketamine/xylazine and partially shaved to expose the surgical site. Surgical sites were sterilized with betadine and alcohol, and lateral incisions were made in the skin between the knee joint and the elbow joint. Sutures were placed connecting the knee and elbow joints of the two mice for anchoring. Skin was aligned between the two mice and sutured from one mouse to the other to close the incision site. Buprenorphine was administered for analgesia for the first 48 h after surgery. Wet food, dry food, and water were provided on the floor of the cage. As needed, mice were supplemented with physiological saline to prevent dehydration. In some experiments, starting on day 14 after surgery, mouse pairs were treated with vehicle (0.1% BSA in PBS) or rIL-33 (2 µg) twice weekly via retroorbital injection into the right eye of the CD45.2^{+} WT mouse for four consecutive weeks.

Statistics

Statistical analyses were performed using GraphPad Prism v.5. Unpaired *t* test or one-way ANOVA with Bonferroni post-test were used to determine statistical significance, as appropriate. When measured values were below the limit of detection, samples were assigned a value at half of the limit of detection to allow for statistical comparisons.

Online supplemental material

Fig. S1 shows cell quantification, CCR3, or CXCR4 expression for major cell lineages in the bone marrow of *St2*$^{-/-}$, rIL-33–treated, and *Alternaria* extract–treated mice. Fig. S2 shows the frequency and total number of ILC2Ps in the bone marrow and ILC2s in the lungs of *Tslpr*$^{-/-}$ mice. Fig. S3 shows flow cytometry gating strategies for LMPPs, CLPs, CHILPs, and ILCPs. Fig. S4 shows the number of ILC2s and the quantification of their cytokine products IL-5 and IL-13 in the lungs of *Alternaria* extract–treated mice. Fig. S5 shows the surface expression of CD90, ST2, and ICOS on ILC2Ps/ILC2s in the bone marrow, lungs, skin, and mLNs. Table S1 lists flow cytometry and FACS antibodies. Table S2 lists quantitative PCR primers. Table S3 lists flow cytometry gating strategies.

ACKNOWLEDGMENTS

We thank Melissa Bloodworth, Weisong Zhou, Hubaida Fuseini, Shinji Toki, and Rachel Brown for their critical insights on this manuscript and data. We are grateful to Dr. Andrew McKenzie for providing us with *Il33*$^{-/-}$ and *St2*$^{-/-}$ mice. We appreciate the

assistance of Kevin Weller, David Flaherty, Brittany Matlock, and Chris Warren in the Vanderbilt University Medical Center Flow Cytometry Shared Resource.

This research was supported by NIH grant R01 AI 111820, NIH grant R01 AI 124456, Department of Veterans Affairs grant 2I01 BX000624, and NIH grant U19 AI 095227 to R. Stokes Peebles Jr.; NIH grant T32 GM007347 to Vanderbilt Medical Scientist Training Program; and NIH grant F30 AI114262 to M.T. Stier.

The authors declare no competing financial interests.

Author contributions: M.T. Stier designed and performed experiments, analyzed data, and assembled the manuscript. J. Zhang, K. Goleniewska, J.Y. Cephus, and M. Rusznak performed experiments. L. Wu and L. Van Kaer performed experiments and provided intellectual assistance and reagents. B. Zhou provided key reagents. D. Newcomb provided intellectual assistance. R.S. Peebles Jr. provided broad guidance in experimental design, data analysis, and manuscript preparation.

Submitted: 17 April 2017

Revised: 3 October 2017

Accepted: 3 November 2017

REFERENCES

Bahrami Mahneh, S., M. Movahedi, Z. Aryan, M.A. Bahar, A. Rezaei, M. Sadr, and N. Rezaei. Universal Scientific Education and Research Network (USERN). 2015. Serum IL-33 is elevated in children with asthma and is associated with disease severity. *Int. Arch. Allergy Immunol.* 168:193–196. https://doi.org/10.1159/000442413

Bartemes, K.R., and H. Kita. 2012. Dynamic role of epithelium-derived cytokines in asthma. *Clin. Immunol.* 143:222–235. https://doi.org/10.1016/j.clim.2012.03.001

Bartemes, K.R., K. Iijima, T. Kobayashi, G.M. Kephart, A.N. McKenzie, and H. Kita. 2012. IL-33-responsive lineage- CD25+ CD44(hi) lymphoid cells mediate innate type 2 immunity and allergic inflammation in the lungs. *J. Immunol.* 188:1503–1513. https://doi.org/10.4049/jimmunol.1102832

Bartemes, K.R., G.M. Kephart, S.J. Fox, and H. Kita. 2014. Enhanced innate type 2 immune response in peripheral blood from patients with asthma. *J. Allergy Clin. Immunol.* 134:671–678.e4. https://doi.org/10.1016/j.jaci.2014.06.024

Bonanno, A., S. Gangemi, S. La Grutta, V. Malizia, L. Riccobono, P. Colombo, F. Cibella, and M. Profita. 2014. 25-Hydroxyvitamin D, IL-31, and IL-33 in children with allergic disease of the airways. *Mediators Inflamm.* 2014:520241. https://doi.org/10.1155/2014/520241

Bonig, H., K.L. Watts, K.-H. Chang, H.-P. Kiem, and T. Papayannopoulou. 2009. Concurrent blockade of α4-integrin and CXCR4 in hematopoietic stem/progenitor cell mobilization. *Stem Cells.* 27:836–837. https://doi.org/10.1002/stem.9

Brestoff, J.R., B.S. Kim, S.A. Saenz, R.R. Stine, L.A. Monticelli, G.F. Sonnenberg, J.J. Thome, D.L. Farber, K. Lutfy, P. Seale, and D. Artis. 2015. Group 2 innate lymphoid cells promote beiging of white adipose tissue and limit obesity. *Nature.* 519:242–246. https://doi.org/10.1038/nature14115

Carpino, N., W.E. Thierfelder, M.S. Chang, C. Saris, S.J. Turner, S.F. Ziegler, and J.N. Ihle. 2004. Absence of an essential role for thymic stromal lymphopoietin receptor in murine B-cell development. *Mol. Cell. Biol.* 24:2584–2592. https://doi.org/10.1128/MCB.24.6.2584-2592.2004

Chang, Y.-J., H.Y. Kim, L.A. Albacker, N. Baumgarth, A.N.J. McKenzie, D.E. Smith, R.H. Dekruyff, and D.T. Umetsu. 2011. Innate lymphoid cells mediate influenza-induced airway hyper-reactivity independently of adaptive immunity. *Nat. Immunol.* 12:631–638. https://doi.org/10.1038/ni.2045

Chauhan, A., M. Singh, A. Agarwal, and N. Paul. 2015. Correlation of TSLP, IL-33, and CD4 + CD25 + FOXP3 + T regulatory (Treg) in pediatric asthma. *J. Asthma.* 52:868–872. https://doi.org/10.3109/02770903.2015.1026441

Christianson, C.A., N.P. Goplen, I. Zafar, C. Irvin, J.T. Good Jr., D.R. Rollins, B. Gorentla, W. Liu, M.M. Gorska, H. Chu, et al. 2015. Persistence of asthma requires multiple feedback circuits involving type 2 innate lymphoid cells and IL-33. *J. Allergy Clin. Immunol.* 136:59–68.e14. https://doi.org/10.1016/j.jaci.2014.11.037

Constantinides, M.G., B.D. McDonald, P.A. Verhoef, and A. Bendelac. 2014. A committed precursor to innate lymphoid cells. *Nature.* 508:397–401. https://doi.org/10.1038/nature13047

de Kleer, I.M., M. Kool, M.J.W. de Bruijn, M. Willart, J. van Moorleghem, M.J. Schuijs, M. Plantinga, R. Beyaert, E. Hams, P.G. Fallon, et al. 2016. Perinatal activation of the interleukin-33 pathway promotes type 2 immunity in the developing lung. *Immunity.* 45:1285–1298. https://doi.org/10.1016/j.immuni.2016.10.031

Doherty, T.A., N. Khorram, S. Lund, A.K. Mehta, M. Croft, and D.H. Broide. 2013. Lung type 2 innate lymphoid cells express cysteinyl leukotriene receptor 1, which regulates TH2 cytokine production. *J. Allergy Clin. Immunol.* 132:205–213. https://doi.org/10.1016/j.jaci.2013.03.048

Drake, L.Y., K. Iijima, and H. Kita. 2014. Group 2 innate lymphoid cells and $CD4^+$ T cells cooperate to mediate type 2 immune response in mice. *Allergy.* 69:1300–1307. https://doi.org/10.1111/all.12446

Drake, L.Y., K. Iijima, K. Bartemes, and H. Kita. 2016. Group 2 innate lymphoid cells promote an early antibody response to a respiratory antigen in mice. *J. Immunol.* 197:1335–1342. https://doi.org/10.4049/jimmunol.1502669

Gasteiger, G., X. Fan, S. Dikiy, S.Y. Lee, and A.Y. Rudensky. 2015. Tissue residency of innate lymphoid cells in lymphoid and nonlymphoid organs. *Science.* 350:981–985. https://doi.org/10.1126/science.aac9593

Ghaedi, M., C.A. Steer, I. Martinez-Gonzalez, T.Y.F. Halim, N. Abraham, and F. Takei. 2016. Common-lymphoid-progenitor-independent pathways of innate and t lymphocyte development. *Cell Reports.* 15:471–480. https://doi.org/10.1016/j.celrep.2016.03.039

Glück, J., B. Rymarczyk, and B. Rogala. 2012. Serum IL-33 but not ST2 level is elevated in intermittent allergic rhinitis and is a marker of the disease severity. *Inflamm. Res.* 61:547–550. https://doi.org/10.1007/s00011-012-0443-9

Gold, M.J., F. Antignano, T.Y.F. Halim, J.A. Hirota, M.-R. Blanchet, C. Zaph, F. Takei, and K.M. McNagny. 2014. Group 2 innate lymphoid cells facilitate sensitization to local, but not systemic, TH2-inducing allergen exposures. *J. Allergy Clin. Immunol.* 133:1142–1148. https://doi.org/10.1016/j.jaci.2014.02.033

Griffith, J.W., C.L. Sokol, and A.D. Luster. 2014. Chemokines and chemokine receptors: Positioning cells for host defense and immunity. *Annu. Rev. Immunol.* 32:659–702. https://doi.org/10.1146/annurev-immunol-032713-120145

Halim, T.Y.F., R.H. Krauss, A.C. Sun, and F. Takei. 2012. Lung natural helper cells are a critical source of Th2 cell-type cytokines in protease allergen-induced airway inflammation. *Immunity.* 36:451–463. https://doi.org/10.1016/j.immuni.2011.12.020

Halim, T.Y.F., C.A. Steer, L. Mathä, M.J. Gold, I. Martinez-Gonzalez, K.M. McNagny, A.N.J. McKenzie, and F. Takei. 2014. Group 2 innate lymphoid cells are critical for the initiation of adaptive T helper 2 cell-mediated allergic lung inflammation. *Immunity.* 40:425–435. https://doi.org/10.1016/j.immuni.2014.01.011

Halim, T.Y.F., Y.Y. Hwang, S.T. Scanlon, H. Zaghouani, N. Garbi, P.G. Fallon, and A.N.J. McKenzie. 2016. Group 2 innate lymphoid cells license dendritic cells to potentiate memory TH2 cell responses. *Nat. Immunol.* 17:57–64. https://doi.org/10.1038/ni.3294

Hardman, C.S., V. Panova, and A.N.J. McKenzie. 2013. IL-33 citrine reporter mice reveal the temporal and spatial expression of IL-33 during allergic lung inflammation. *Eur. J. Immunol.* 43:488–498. https://doi.org/10.1002/eji.201242863

Howitt, M.R., S. Lavoie, M. Michaud, A.M. Blum, S.V. Tran, J.V. Weinstock, C.A. Gallini, K. Redding, R.F. Margolskee, L.C. Osborne, et al. 2016.

Tuft cells, taste-chemosensory cells, orchestrate parasite type 2 immunity in the gut. *Science.* 351:1329–1333. https://doi.org/10.1126/science.aaf1648

Hoyler, T., C.S.N. Klose, A. Souabni, A. Turqueti-Neves, D. Pfeifer, E.L. Rawlins, D. Voehringer, M. Busslinger, and A. Diefenbach. 2012. The transcription factor GATA-3 controls cell fate and maintenance of type 2 innate lymphoid cells. *Immunity.* 37:634–648. https://doi.org/10.1016/j.immuni.2012.06.020

Jackson, D.J., H. Makrinioti, B.M.J. Rana, B.W.H. Shamji, M.-B. Trujillo-Torralbo, J. Footitt, A.G. Jerico Del-Rosario, A.G. Telcian, A. Nikonova, J. Zhu, et al. 2014. IL-33-dependent type 2 inflammation during rhinovirus-induced asthma exacerbations in vivo. *Am. J. Respir. Crit. Care Med.* 190:1373–1382. https://doi.org/10.1164/rccm.201406-1039OC

Karta, M.R., P.S. Rosenthal, A. Beppu, C.Y. Vuong, M. Miller, S. Das, R.C. Kurten, T.A. Doherty, and D.H. Broide. 2017. β2 Integrins rather than β1 integrins mediate alternaria-induced ILC2 trafficking to the lung. *J. Allergy Clin. Immunol.* https://doi.org/10.1016/j.jaci.2017.03.010

Kawai, T., and H.L. Malech. 2009. WHIM syndrome: Congenital immune deficiency disease. *Curr. Opin. Hematol.* 16:20–26. https://doi.org/10.1097/MOH.0b013e32831ac557

Kim, B.S., M.C. Siracusa, S.A. Saenz, M. Noti, L.A. Monticelli, G.F. Sonnenberg, M.R. Hepworth, A.S. Van Voorhees, M.R. Comeau, and D. Artis. 2013. TSLP elicits IL-33-independent innate lymphoid cell responses to promote skin inflammation. *Sci. Transl. Med.* 5:170ra16. https://doi.org/10.1126/scitranslmed.3005374

Klose, C.S.N., and D. Artis. 2016. Innate lymphoid cells as regulators of immunity, inflammation and tissue homeostasis. *Nat. Immunol.* 17:765–774. https://doi.org/10.1038/ni.3489

Klose, C.S.N., M. Flach, L. Möhle, L. Rogell, T. Hoyler, K. Ebert, C. Fabiunke, D. Pfeifer, V. Sexl, D. Fonseca-Pereira, et al. 2014. Differentiation of type 1 ILCs from a common progenitor to all helper-like innate lymphoid cell lineages. *Cell.* 157:340–356. https://doi.org/10.1016/j.cell.2014.03.030

Lee, M.-W., J.I. Odegaard, L. Mukundan, Y. Qiu, A.B. Molofsky, J.C. Nussbaum, K. Yun, R.M. Locksley, and A. Chawla. 2015. Activated type 2 innate lymphoid cells regulate beige fat biogenesis. *Cell.* 160:74–87. https://doi.org/10.1016/j.cell.2014.12.011

Li, D., R. Guabiraba, A.-G. Besnard, M. Komai-Koma, M.S. Jabir, L. Zhang, G.J. Graham, M. Kurowska-Stolarska, F.Y. Liew, C. McSharry, and D. Xu. 2014. IL-33 promotes ST2-dependent lung fibrosis by the induction of alternatively activated macrophages and innate lymphoid cells in mice. *J. Allergy Clin. Immunol.* 134:1422–1432.e11. https://doi.org/10.1016/j.jaci.2014.05.011

Mackley, E.C., S. Houston, C.L. Marriott, E.E. Halford, B. Lucas, V. Cerovic, K.J. Filbey, R.M. Maizels, M.R. Hepworth, G.F. Sonnenberg, et al. 2015. CCR7-dependent trafficking of RORγ$^+$ ILCs creates a unique microenvironment within mucosal draining lymph nodes. *Nat. Commun.* 6:5862. https://doi.org/10.1038/ncomms6862

Matsuyama, Y., H. Okazaki, H. Tamemoto, H. Kimura, Y. Kamata, K. Nagatani, T. Nagashima, M. Hayakawa, M. Iwamoto, T. Yoshio, et al. 2010. Increased levels of interleukin 33 in sera and synovial fluid from patients with active rheumatoid arthritis. *J. Rheumatol.* 37:18–25. https://doi.org/10.3899/jrheum.090492

Miller, A.M. 2011. Role of IL-33 in inflammation and disease. *J. Inflamm. (Lond.).* 8:22. https://doi.org/10.1186/1476-9255-8-22

Mirchandani, A.S., A.-G. Besnard, E. Yip, C. Scott, C.C. Bain, V. Cerovic, R.J. Salmond, and F.Y. Liew. 2014. Type 2 innate lymphoid cells drive CD4+ Th2 cell responses. *J. Immunol.* 192:2442–2448. https://doi.org/10.4049/jimmunol.1300974

Mitsui, A., Y. Tada, T. Takahashi, S. Shibata, M. Kamata, T. Miyagaki, H. Fujita, M. Sugaya, T. Kadono, S. Sato, and Y. Asano. 2016. Serum IL-33 levels are increased in patients with psoriasis. *Clin. Exp. Dermatol.* 41:183–189. https://doi.org/10.1111/ced.12670

Mjösberg, J.M., S. Trifari, N.K. Crellin, C.P. Peters, C.M. van Drunen, B. Piet, W.J. Fokkens, T. Cupedo, and H. Spits. 2011. Human IL-25- and IL-33-responsive type 2 innate lymphoid cells are defined by expression of CRTH2 and CD161. *Nat. Immunol.* 12:1055–1062. https://doi.org/10.1038/ni.2104

Mjösberg, J., J. Bernink, K. Golebski, J.J. Karrich, C.P. Peters, B. Blom, A.A. te Velde, W.J. Fokkens, C.M. van Drunen, and H. Spits. 2012. The transcription factor GATA3 is essential for the function of human type 2 innate lymphoid cells. *Immunity.* 37:649–659. https://doi.org/10.1016/j.immuni.2012.08.015

Molofsky, A.B., J.C. Nussbaum, H.-E. Liang, S.J. Van Dyken, L.E. Cheng, A. Mohapatra, A. Chawla, and R.M. Locksley. 2013. Innate lymphoid type 2 cells sustain visceral adipose tissue eosinophils and alternatively activated macrophages. *J. Exp. Med.* 210:535–549. https://doi.org/10.1084/jem.20121964

Monticelli, L.A., G.F. Sonnenberg, M.C. Abt, T. Alenghat, C.G.K. Ziegler, T.A. Doering, J.M. Angelosanto, B.J. Laidlaw, C.Y. Yang, T. Sathaliyawala, et al. 2011. Innate lymphoid cells promote lung-tissue homeostasis after infection with influenza virus. *Nat. Immunol.* 12:1045–1054. https://doi.org/10.1038/ni.2131

Monticelli, L.A., L.C. Osborne, M. Noti, S.V. Tran, D.M.W. Zaiss, and D. Artis. 2015. IL-33 promotes an innate immune pathway of intestinal tissue protection dependent on amphiregulin-EGFR interactions. *Proc. Natl. Acad. Sci. USA.* 112:10762–10767. https://doi.org/10.1073/pnas.1509070112

Morita, H., K. Moro, and S. Koyasu. 2016. Innate lymphoid cells in allergic and nonallergic inflammation. *J. Allergy Clin. Immunol.* 138:1253–1264. https://doi.org/10.1016/j.jaci.2016.09.011

Moro, K., T. Yamada, M. Tanabe, T. Takeuchi, T. Ikawa, H. Kawamoto, J. Furusawa, M. Ohtani, H. Fujii, and S. Koyasu. 2010. Innate production of T(H)2 cytokines by adipose tissue-associated c-Kit(+)Sca-1(+) lymphoid cells. *Nature.* 463:540–544. https://doi.org/10.1038/nature08636

Moro, K., H. Kabata, M. Tanabe, S. Koga, N. Takeno, M. Mochizuki, K. Fukunaga, K. Asano, T. Betsuyaku, and S. Koyasu. 2016. Interferon and IL-27 antagonize the function of group 2 innate lymphoid cells and type 2 innate immune responses. *Nat. Immunol.* 17:76–86. https://doi.org/10.1038/ni.3309

Mu, R., H.-Q. Huang, Y.-H. Li, C. Li, H. Ye, and Z.-G. Li. 2010. Elevated serum interleukin 33 is associated with autoantibody production in patients with rheumatoid arthritis. *J. Rheumatol.* 37:2006–2013. https://doi.org/10.3899/jrheum.100184

Neill, D.R., S.H. Wong, A. Bellosi, R.J. Flynn, M. Daly, T.K.A. Langford, C. Bucks, C.M. Kane, P.G. Fallon, R. Pannell, et al. 2010. Nuocytes represent a new innate effector leukocyte that mediates type-2 immunity. *Nature.* 464:1367–1370. https://doi.org/10.1038/nature08900

Nussbaum, J.C., S.J. Van Dyken, J. von Moltke, L.E. Cheng, A. Mohapatra, A.B. Molofsky, E.E. Thornton, M.F. Krummel, A. Chawla, H.-E. Liang, and R.M. Locksley. 2013. Type 2 innate lymphoid cells control eosinophil homeostasis. *Nature.* 502:245–248. https://doi.org/10.1038/nature12526

O'Sullivan, T.E., M. Rapp, X. Fan, O.-E. Weizman, P. Bhardwaj, N.M. Adams, T. Walzer, A.J. Dannenberg, and J.C. Sun. 2016. Adipose-resident group 1 innate lymphoid cells promote obesity-associated insulin resistance. *Immunity.* 45:428–441. https://doi.org/10.1016/j.immuni.2016.06.016

Oboki, K., T. Ohno, N. Kajiwara, K. Arae, H. Morita, A. Ishii, A. Nambu, T. Abe, H. Kiyonari, K. Matsumoto, et al. 2010. IL-33 is a crucial amplifier of innate rather than acquired immunity. *Proc. Natl. Acad. Sci. USA.* 107:18581–18586. https://doi.org/10.1073/pnas.1003059107

Oliphant, C.J., Y.Y. Hwang, J.A. Walker, M. Salimi, S.H. Wong, J.M. Brewer, A. Englezakis, J.L. Barlow, E. Hams, S.T. Scanlon, et al. 2014. MHCII-mediated dialog between group 2 innate lymphoid cells and CD4(+) T cells potentiates type 2 immunity and promotes parasitic helminth

expulsion. *Immunity.* 41:283–295. https://doi.org/10.1016/j.immuni.2014.06.016

Pastorelli, L., R.R. Garg, S.B. Hoang, L. Spina, B. Mattioli, M. Scarpa, C. Fiocchi, M. Vecchi, and T.T. Pizarro. 2010. Epithelial-derived IL-33 and its receptor ST2 are dysregulated in ulcerative colitis and in experimental Th1/Th2 driven enteritis. *Proc. Natl. Acad. Sci. USA.* 107:8017–8022. https://doi.org/10.1073/pnas.0912678107

Petty, J.M., C.C. Lenox, D.J. Weiss, M.E. Poynter, and B.T. Suratt. 2009. Crosstalk between CXCR4/stromal derived factor-1 and VLA-4/VCAM-1 pathways regulates neutrophil retention in the bone marrow. *J. Immunol.* 182:604–612. https://doi.org/10.4049/jimmunol.182.1.604

Price, A.E., H.-E. Liang, B.M. Sullivan, R.L. Reinhardt, C.J. Eisley, D.J. Erle, and R.M. Locksley. 2010. Systemically dispersed innate IL-13-expressing cells in type 2 immunity. *Proc. Natl. Acad. Sci. USA.* 107:11489–11494. https://doi.org/10.1073/pnas.1003988107

Saadah, O.I., S.E. Al-Harthi, J.A. Al-Mughales, Y.Y. Bin-Taleb, and R.S. Baeshen. 2015. Serum interleukin-33 level in Saudi children with inflammatory bowel disease. *Int. J. Clin. Exp. Pathol.* 8:16000–16006.

Salimi, M., J.L. Barlow, S.P. Saunders, L. Xue, D. Gutowska-Owsiak, X. Wang, L.-C. Huang, D. Johnson, S.T. Scanlon, A.N.J. McKenzie, et al. 2013. A role for IL-25 and IL-33-driven type-2 innate lymphoid cells in atopic dermatitis. *J. Exp. Med.* 210:2939–2950. https://doi.org/10.1084/jem.20130351

Salo, P.M., S.J. Arbes Jr., M. Sever, R. Jaramillo, R.D. Cohn, S.J. London, and D.C. Zeldin. 2006. Exposure to Alternaria alternata in US homes is associated with asthma symptoms. *J. Allergy Clin. Immunol.* 118:892–898. https://doi.org/10.1016/j.jaci.2006.07.037

Saluzzo, S., A.-D. Gorki, B.M.J. Rana, R. Martins, S. Scanlon, P. Starkl, K. Lakovits, A. Hladik, A. Korosec, O. Sharif, et al. 2017. First-breath-induced type 2 pathways shape the lung immune environment. *Cell Reports.* 18:1893–1905. https://doi.org/10.1016/j.celrep.2017.01.071

Shaw, J.L., S. Fakhri, M.J. Citardi, P.C. Porter, D.B. Corry, F. Kheradmand, Y.-J. Liu, and A. Luong. 2013. IL-33-responsive innate lymphoid cells are an important source of IL-13 in chronic rhinosinusitis with nasal polyps. *Am. J. Respir. Crit. Care Med.* 188:432–439. https://doi.org/10.1164/rccm.201212-2227OC

Spooner, C.J., J. Lesch, D. Yan, A.A. Khan, A. Abbas, V. Ramirez-Carrozzi, M. Zhou, R. Soriano, J. Eastham-Anderson, L. Diehl, et al. 2013. Specification of type 2 innate lymphocytes by the transcriptional determinant Gfi1. *Nat. Immunol.* 14:1229–1236. https://doi.org/10.1038/ni.2743

Steer, C.A., I. Martinez-Gonzalez, M. Ghaedi, P. Allinger, L. Mathä, and F. Takei. 2017. Group 2 innate lymphoid cell activation in the neonatal lung drives type 2 immunity and allergen sensitization. *J. Allergy Clin. Immunol.* 140:593–595.e3. https://doi.org/10.1016/j.jaci.2016.12.984

Stier, M.T., M.H. Bloodworth, S. Toki, D.C. Newcomb, K. Goleniewska, K.L. Boyd, M. Quitalig, A.L. Hotard, M.L. Moore, T.V. Hartert, et al. 2016. Respiratory syncytial virus infection activates IL-13-producing group 2 innate lymphoid cells through thymic stromal lymphopoietin. *J. Allergy Clin. Immunol.* 138:814–824.e11. https://doi.org/10.1016/j.jaci.2016.01.050

Tamagawa-Mineoka, R., Y. Okuzawa, K. Masuda, and N. Katoh. 2014. Increased serum levels of interleukin 33 in patients with atopic dermatitis. *J. Am. Acad. Dermatol.* 70:882–888. https://doi.org/10.1016/j.jaad.2014.01.867

Townsend, M.J., P.G. Fallon, D.J. Matthews, H.E. Jolin, and A.N. McKenzie. 2000. T1/ST2-deficient mice demonstrate the importance of T1/ST2 in developing primary T helper cell type 2 responses. *J. Exp. Med.* 191:1069–1076. https://doi.org/10.1084/jem.191.6.1069

Vandesompele, J., K. De Preter, F. Pattyn, B. Poppe, N. Van Roy, A. De Paepe, and F. Speleman. 2002. Accurate normalization of real-time quantitative RT-PCR data by geometric averaging of multiple internal control genes. *Genome Biol.* 3:RESEARCH0034.

Vély, F., V. Barlogis, B. Vallentin, B. Neven, C. Piperoglou, M. Ebbo, T. Perchet, M. Petit, N. Yessaad, F. Touzot, et al. 2016. Evidence of innate lymphoid cell redundancy in humans. *Nat. Immunol.* 17:1291–1299. https://doi.org/10.1038/ni.3553

von Moltke, J., M. Ji, H.-E. Liang, and R.M. Locksley. 2016. Tuft-cell-derived IL-25 regulates an intestinal ILC2-epithelial response circuit. *Nature.* 529:221–225. https://doi.org/10.1038/nature16161

Walker, J.A., C.J. Oliphant, A. Englezakis, Y. Yu, S. Clare, H.-R. Rodewald, G. Belz, P. Liu, P.G. Fallon, and A.N.J. McKenzie. 2015. Bcl11b is essential for group 2 innate lymphoid cell development. *J. Exp. Med.* 212:875–882. https://doi.org/10.1084/jem.20142224

Wilhelm, C., K. Hirota, B. Stieglitz, J. Van Snick, M. Tolaini, K. Lahl, T. Sparwasser, H. Helmby, and B. Stockinger. 2011. An IL-9 fate reporter demonstrates the induction of an innate IL-9 response in lung inflammation. *Nat. Immunol.* 12:1071–1077. https://doi.org/10.1038/ni.2133

Wong, S.H., J.A. Walker, H.E. Jolin, L.F. Drynan, E. Hams, A. Camelo, J.L. Barlow, D.R. Neill, V. Panova, U. Koch, et al. 2012. Transcription factor RORα is critical for nuocyte development. *Nat. Immunol.* 13:229–236. https://doi.org/10.1038/ni.2208

Xu, W., R.G. Domingues, D. Fonseca-Pereira, M. Ferreira, H. Ribeiro, S. Lopez-Lastra, Y. Motomura, L. Moreira-Santos, F. Bihl, V. Braud, et al. 2015. NFIL3 orchestrates the emergence of common helper innate lymphoid cell precursors. *Cell Reports.* 10:2043–2054. https://doi.org/10.1016/j.celrep.2015.02.057

Xue, L., M. Salimi, I. Panse, J.M. Mjösberg, A.N.J. McKenzie, H. Spits, P. Klenerman, and G. Ogg. 2014. Prostaglandin D2 activates group 2 innate lymphoid cells through chemoattractant receptor-homologous molecule expressed on TH2 cells. *J. Allergy Clin. Immunol.* 133:1184–1194. https://doi.org/10.1016/j.jaci.2013.10.056

Yu, X., R. Pappu, V. Ramirez-Carrozzi, N. Ota, P. Caplazi, J. Zhang, D. Yan, M. Xu, W.P. Lee, and J.L. Grogan. 2014. TNF superfamily member TL1A elicits type 2 innate lymphoid cells at mucosal barriers. *Mucosal Immunol.* 7:730–740. https://doi.org/10.1038/mi.2013.92

Yu, Y., C. Wang, S. Clare, J. Wang, S.-C. Lee, C. Brandt, S. Burke, L. Lu, D. He, N.A. Jenkins, et al. 2015. The transcription factor Bcl11b is specifically expressed in group 2 innate lymphoid cells and is essential for their development. *J. Exp. Med.* 212:865–874. https://doi.org/10.1084/jem.20142318

Zhou, B., M.R. Comeau, T. De Smedt, H.D. Liggitt, M.E. Dahl, D.B. Lewis, D. Gyarmati, T. Aye, D.J. Campbell, and S.F. Ziegler. 2005. Thymic stromal lymphopoietin as a key initiator of allergic airway inflammation in mice. *Nat. Immunol.* 6:1047–1053. https://doi.org/10.1038/ni1247

Zhou, W., S. Toki, J. Zhang, K. Goleniewksa, D.C. Newcomb, J.Y. Cephus, D.E. Dulek, M.H. Bloodworth, M.T. Stier, V. Polosuhkin, et al. 2016. Prostaglandin I2 signaling and inhibition of group 2 innate lymphoid cell responses. *Am. J. Respir. Crit. Care Med.* 193:31–42. https://doi.org/10.1164/rccm.201410-1793OC

Zook, E.C., and B.L. Kee. 2016. Development of innate lymphoid cells. *Nat. Immunol.* 17:775–782. https://doi.org/10.1038/ni.3481

Zook, E.C., K. Ramirez, X. Guo, G. van der Voort, M. Sigvardsson, E.C. Svensson, Y.-X. Fu, and B.L. Kee. 2016. The ETS1 transcription factor is required for the development and cytokine-induced expansion of ILC2. *J. Exp. Med.* 213:687–696. https://doi.org/10.1084/jem.20150851